OSCILLATORY BEHAVIOR IN AN OCEAN GENERAL CIRCULATION MODEL OF THE NORTH ATLANTIC

by

Catherine Alicia Brown

A thesis submitted in conformity with the requirements
for the degree of Master of Science
Graduate Department of Geography
University of Toronto

The author has granted a non-exclusive licence allowing the National Library of Canada to reproduce, loan, distribute or sell copies of this thesis in microform, paper or electronic formats.

The author retains ownership of the copyright in this thesis. Neither the thesis nor substantial extracts from it may be printed or otherwise reproduced without the author's permission.

L'auteur a accordé une licence non exclusive permettant à la Bibliothèque nationale du Canada de reproduire, prêter, distribuer ou vendre des copies de cette thèse sous la forme de microfiche/film, de reproduction sur papier ou sur format électronique.

L'auteur conserve la propriété du droit d'auteur qui protège cette thèse. Ni la thèse ni des extraits substantiels de celle-ci ne doivent être imprimés ou autrement reproduits sans son autorisation.

0-612-46006-1

Canada

Abstract

Coarse resolution ocean general circulation models are known to produce oscillatory behavior in a variety of forms and over a spectrum of timescales. There are four main potential sources for this behavior: internal model parameters (diffusivities, viscosities), external forcing (wind stress, thermal forcing, freshwater forcing), topography, and initial conditions. After imposing enhanced salinity fluxes with mixed boundary conditions, the model simulations produced a spectrum of oscillatory behavior as a function of the internal modeling parameters alone. In this study, the experiments with idealized topography generated a wider range of model behavior than reported in other studies. In general, this work has shown that two dimensional salinity fluxes produced a broader range of behavior than described in the literature where idealized salinity fluxes trivialized the variability of the diagnosed salt flux field. The initial conditions were the least important of the factors effecting the thermohaline circulation.

Acknowledgments

I would like to thank my supervisor, Professor W. Gough, for his encouragement and support throughout the course of this study. The Climate Lab is a wonderful research environment and I have thoroughly enjoyed sharing this experience with fellow 'climate labbers' over the years. Thanks to Professor W. Welch for sharing his expertise in statistical methods. I also wish to gratefully acknowledge Derek Wyatt for his generous assistance and guidance with computer issues of all nature.

I sincerely thank my family and friends for their constant love and encouragement. I would like to thank Kevin for his thoughtful advice and support over the years. Thanks to my dear sisters, Colleen and Heather, for sharing their laughter and inspiration. Grateful acknowledgment to my mother, Violeta, for her guidance and moral support. Finally, special thanks to my father, Ian, whose patience, humor and advice are always cherished.

Table of Contents

List of Tables

List of Figures

1. Introduction

1.1 The thermohaline circulation as component of the climate system and multiple equilibria

In the present climate, the meridional heat transport by the oceans toward the North Atlantic across 24^0N is approximately 1.2 PW (1 PW = $10^{15}W$) (Roemmich and Wunsch 1984). The climatic effect of this thermohaline flow pattern is demonstrated by the 4-5^{0}C warmer surface temperatures of the northern Atlantic compared to the same latitudes in the Pacific. The Broecker (1987) and Gordon (1986) descriptions of the thermohaline circulation as a conveyor belt graphically emphasized the interconnections between the waters of the world's oceans. The thermohaline circulation in the Atlantic consists of two parts: 1) northward flow of warm water, termed the upper limb, (some of this water contributes to the production of new deep water in the high latitudes of the North Atlantic); and 2) southward export of newly formed deep water, referred to as the lower limb. The thermohaline circulation differs from the wind-driven circulation in that the former is forced by density differences that are controlled by changes in temperature and salinity. During the winter in the high latitudes of the North Atlantic, the water column becomes unstable due to a combination of intensive cooling at the ocean surface from the passage of winter storms, northward transport of salty surface water from lower latitudes, and brine rejection when ice forms. All of these factors increase the density of the surface waters. Consequently, the water column convects, and mixes vertically. This newly formed water is carried southward at abyssal depths along the western boundary in the lower limb of the thermohaline circulation. In summary, this flow is driven by surface heat and freshwater (buoyancy) fluxes, and it is typically thermally direct (heat fluxes dominate) such that the densest surface waters are found in cold high-latitude regions, not in the salty subtropics. This thermally driven overturning can be halted by high latitude excess of precipitation over evaporation and low latitude excess evaporation over precipitation (except in a relatively narrow belt at the Intertropical Convergence Zone).

The ocean is an important regulator of climate due to its large thermal inertia and its potential to store both anthropogenic and natural greenhouse gases (Weaver and Hughes 1992); however, the ocean circulation has much more than just a damping effect on climatic changes. Investigation of the complex stability properties of the thermohaline circulation has led to the ocean becoming a prime suspect for some of the erratic behavior recorded in past

climate records preserved in the Greenland Ice Sheet and in oceanic sediments. The competing properties of temperature and salinity in the net 'surface buoyancy forcing of the ocean' are the key determinants of multiple equilibria and stability and variability properties of the thermohaline circulation. Experiments with three-dimensional ocean models with idealized basin geometry have confirmed that thermohaline variability can exist even in the presence of constant atmospheric forcing, both at decadal and at longer time scales. The existence of multiple steady states, when different boundary conditions are applied, has been established in models ranging in sophistication from two-box models to global general circulation models (Weaver and Hughes 1992). Stommel's (1961) classical box model introduced the fundamental mechanism responsible for multiple equilibria which is the positive salt advection feedback. The advection of heat and salt by the thermohaline circulation is determined by the pole-to-equator density difference. Lower salinity in high latitudes dampens the thermally direct circulation, reducing the poleward transport of more saline water, and is thus a positive feedback. The box model has two stable equilibrium states for weak net precipitation in high latitudes such as today's climate: 1) a fast, thermally dominated solution; and, 2) a slow reverse circulation (haline dominated with sinking in the tropics).

Several researchers have speculated that variations in the ocean circulation, on decadal and longer time scales, may be one of the prime causes of rapid and drastic natural climate swings (Broecker et al. 1985). Paleoclimatological research shows that the formation of North Atlantic Deep Water was repeatedly interrupted or reduced in glacial times, leading to abrupt climatic changes in the North Atlantic region (Boyle and Keigwin 1987; Broecker 1991; Keigwin et al. 1991). Results from the GISP-2 ice core in Greenland (Taylor et al. 1993) indicate Pleistocene climate changes between glacial and near-interglacial conditions in periods of less than a decade. Such rapid climate fluctuations have occurred not only during the past glacial but very likely in the Eemian interglacial and the previous Saale-Holstein glacial cycle (Dansgaard et al. 1993; GRIP Members 1993). These data suggest that the stable conveyor belt circulation of the past 10 000 years is an exception rather than the rule. The observed fluctuations in the Eemian, which was warmer than the present, raise concerns about whether global warming could destabilize the deep circulation. Analysis of hydrographic and other data has shown that the coupled ocean-atmosphere system is variable on decadal time scales (Deser and Blackmon 1993; Kushnir 1994; Hansen and Bezdek 1996; Reverdin et al.

1997). In order to determine whether the increasing concentration of greenhouse gases is affecting our climate, an understanding is required of natural climate variability due to changes of ocean circulation.

In ocean model simulations, the dramatic flushing events that characterize millennial scale oscillations – with heat accumulated by the ocean over centuries being released in a few years (Marotzke et al. 1988; Weaver and Sarachik 1991a,b) – suggest a possible connection with rapid glacial-to-interglacial transitions. Oscillations with periods of thousands of years are supported by the analysis of paleo-oceanographic data (Broecker et al. 1985; Yiou et al. 1994). Carrying this connection further, some authors have associated the interdecadal-to-centennial oscillations found in the relaxation stage of the millennial oscillation with the Heinrich (1988) events affecting the North Atlantic thermohaline circulation over the last full glacial cycle (Broecker et al. 1992; Bond et al. 1993; Grousset et al. 1993). Inclusion of a sea ice component will be necessary to explore these possibilities further. Thermohaline circulation stability has been reviewed by Weaver and Hughes (1992) and Rahmstorf et al. (1996).

1.2 Oscillations in ocean modeling

1.2.1 Representation of the atmosphere by surface boundary conditions

The oceanic general circulation is forced by wind stress, surface heating and cooling, and exchange of fresh water with the atmosphere. A fully prognostic atmospheric model is computationally very expensive and often is not included in models for ocean climate studies. The coupled system can be modeled as a dynamical ocean model with the response of the atmosphere represented by a simple diagnostic parameterization (Bretherton 1982; Hasselmann 1991). In this way, climate changes in the ocean can be studied whereby the coupling to the atmosphere is prescribed by a surface boundary condition representing a crude model of atmospheric behavior. The type of surface boundary condition chosen to represent the atmosphere will have an important influence on the ocean circulation and feedbacks in the coupled system.

1.2.1.1 Restoring boundary conditions and mixed boundary conditions

To allow some feedback between ocean temperatures and surface heat flux, a restoring boundary condition is commonly used in which the surface temperature of the model ocean is

continuously restored to some fixed effective temperature, which is called the restoring temperature (Haney 1971). A simple, linear, Newtonian damping boundary condition can be used due to the dependence of longwave emission, sensible heating and evaporation (hence latent heat fluxes) on temperature. The upper layer of the ocean is typically restored to an appropriate reference temperature on a fast time scale of 1-2 months. This restoring boundary condition takes the form of a variable flux (in Watts m^{-2}). This approach is commonly referred to as 'Haney restoring boundary conditions' and is used to spin up ocean models to an equilibrium state. An important point to consider is that this parameterization implies a model of an atmosphere whose temperature always remains fixed. It is therefore clear that the restoring boundary condition as suggested by Haney was not intended to be used for climate variability experiments. Other formulations have been suggested such as Rahmstorf and Willebrand (1995) which represent the atmospheric heat transport parametrically and may have a somewhat wider range of validity. Imposing boundary conditions that parameterize the atmospheric feedbacks more realistically and investigating their impact on the variability of the thermohaline circulation has been the focus of several studies (Rahmstorf 1994; Cai and Godfrey 1995; Chen and Ghil 1995).

Freshwater fluxes at the ocean surface which are due to evaporation, precipitation, river runoff, or ice changes may be represented in ocean models as a surface boundary condition on salinity. Evaporation is mainly a function of the air-sea temperature difference while the distribution of precipitation depends on complex small- and large-scale atmospheric processes. The restoring condition on salinity incorrectly implies that the amount of precipitation or evaporation at any given place depends upon the local sea surface salinity. In uncoupled models, this problem is typically resolved by imposing either specified salinity fluxes or a salinity flux which depends weakly on the atmosphere-ocean temperature difference (Weaver and Hughes 1992). Many researchers have used mixed boundary conditions (i.e., a restoring boundary condition on temperature and a flux boundary condition on salinity) to drive ocean models. Since sea-surface salinity is known more accurately than surface freshwater fluxes, the implementation of mixed boundary conditions is usually preceded by a spin up phase in which the model surface salinity is also restored toward a given salinity field. At the equilibrium by the end of this spin up phase, a freshwater flux is diagnosed from the restoring term and used to force the model surface salinity. At this point the sea surface salinity is free to evolve. If the final state of the restoring boundary condition

case were stable under a switch to mixed boundary conditions, then no change in the model computed solution should occur. Instead, many different kinds of behavior have been found, ranging from the polar halocline catastrophe (Bryan 1986a,b) (described below, Section 1.2.2), to "flushes" (Marotzke 1989; Weaver and Sarachik 1991b), low frequency oscillations (Marotzke 1989), and decadal time-scale oscillations (Weaver and Sarachik 1991a).

1.2.1.2 Fixed flux boundary conditions

The recent finding of internal decadal scale variability in models forced only with fixed buoyancy fluxes allows for the possibility that this kind of variability is not truly thermohaline (i.e., does not involve the interplay of heat and salt). The fixed flux experiment is a simplification of the original mixed boundary conditions experiment that retains the timescale of the original variability as well as the prominence of slow boundary-propagating disturbances (Greatbatch and Peterson 1996). The former experiment is obtained from the latter by fixing the heat as well as the salt flux (double flux). Assuming a linear equation of state (its nonlinearity is not important here), the problem can be recast in terms of a single buoyancy variable (single flux).

The relatively long timescale of interdecadal oscillations suggests a fundamental oceanic contribution. Coupled atmosphere-ocean models have reproduced observed patterns of interdecadal variability involving the thermohaline circulation (Delworth et al. 1993). A dynamical atmospheric component does not seem necessary to reproduce this variability since Greatbatch and Zhang (1995) found very similar oscillations in an idealized ocean basin forced by constant heat fluxes. Decadal oscillations have also been described previously in ocean models forced with mixed boundary conditions (Weaver and Sarachik 1991b), but such boundary conditions do not properly represent the large scale atmosphere-ocean interactions (Zhang et al. 1993). Consequently, several studies have analyzed the variability in noncoupled ocean models forced by fixed surface fluxes. Numerous ocean models forced by constant flux boundary conditions for both temperature and salinity were found to generate purely oceanic decadal-scale variability (Huang and Chou 1994; Chen and Ghil 1995; Winton 1996; Greatbatch and Peterson 1996).

Huck et al. (1999) employ only temperature as a simple means to deal with density such that the heat forcing should be considered as a global buoyancy term. They performed an extensive parameter sensitivity analysis of the oscillatory behavior and found that the

oscillations stand out as a robust geostrophic feature whose amplitude is mainly controlled by the horizontal diffusivity. Various experiments with different geometry and forcings were conducted and did not support the necessity of viscous numerical boundary waves or any boundary in sustaining the oscillations.

1.2.2 The polar halocline catastrophe

An abrupt change often demonstrated in ocean circulation simulations is the polar halocline catastrophe. This event marks the switch between polar sinking with convection in polar regions, and equatorial sinking with no polar convection. Several researchers have described the internal oscillation between these states including in two- dimensional (zonally averaged) models (Wright and Stocker 1991), three dimensional frictional geostrophic models (Winton and Sarachik 1993; Zhang et al. 1993), and in the Bryan-Cox primitive equation ocean general circulation model (Bryan 1986b).

Bryan (1986b) demonstrated that multiple equilibria of the thermohaline circulation could exist in a two-hemisphere, three-dimensional ocean general circulation model forced by symmetric mixed boundary conditions and wind stress. The ocean general circulation model was spun up to equilibrium under restoring boundary conditions and then the salt flux required to maintain this steady state was diagnosed and mixed boundary conditions were imposed (Bryan 1986b). The steady state attained by the restoring condition was unstable under mixed boundary conditions and a polar halocline catastrophe resulted. This involved the artificial generation of a freshwater cap at high latitudes that slowly moved towards the equator until a complete collapse of the thermohaline circulation occurred a few decades later (Bryan 1986a). By adding two psu of salt to the high latitude regions of both hemispheres immediately upon switching to mixed boundary conditions, Bryan (1986a,b) was able to obtain a stable, symmetric two-cell equilibrium under mixed boundary conditions. Bryan's (1986a,b) perturbation experiments demonstrated mechanisms such as the convective feedback and advective feedback (described in Section 2.3) and have since become key concepts in our understanding of multiple equilibria. Bryan (1986a, b) discovered that small, finite-amplitude perturbations to the surface salinity budget could induce rapid transitions between equilibria. He also showed that sudden changes in the deep water formation rates were possible, not only in box models, but also in general circulation models, giving more

weight to Broecker's et al.'s (1985) speculation (see Section 1.1). Great interest in these phenomena arises because of their implications for climate variability.

Broecker and Denton (1990) discuss the possibility that transitions in and out of periods of glaciation were accompanied by major reorganizations of the atmosphere-ocean system and of the ocean circulation in particular. The reason the ocean is important is because of its ability to store and transport heat. Recent work has been directed at examining the robustness of this behavior as the surface boundary conditions on the model are made more realistic. For example, Weaver et al. (1993) have shown that including a stochastic component to the surface freshwater flux increases the frequency of 'flushes' and decreases their intensity. These authors have also shown that the structure of the surface freshwater flux is very important for determining the behavior of a model upon a switch to mixed boundary conditions. In particular, strong high latitude freshening seems to be important for a polar halocline catastrophe to occur. Zhang et al. (1993) suggest that the damping time scale for sea surface temperature anomalies should be of the order of hundreds of days, which would lead to less temporal variability of the ocean to atmosphere heat flux. This, in turn, would make that polar halocline catastrophe harder to trigger. Zhang et al. (1993) also demonstrate that the polar halocline catastrophe is less likely to occur if the surface to atmosphere heat flux is held fixed, corresponding to an infinitely long damping time scale.

Results from ocean-only models must be treated with considerable caution as the response of the atmospheric circulation to changes in the ocean is neglected. In ocean-only models one is limited to using approximations through the parameterization for the thermal surface boundary condition. It is rather obvious that the atmosphere would show a dramatic response to a basin-averaged heating of more that $100 \ Wm^{-2}$ which is associated with a flush. This remark also applies to other forms of ocean variability where the atmospheric response may be less dramatic but nevertheless important. Rahmstorf and Willebrand (1995) demonstrated that changes in surface temperature are crucial for the behavior of the thermohaline circulation and should not be neglected. They described a negative temperature advection feedback with a generally stabilizing influence on the thermohaline circulation. This feedback depends heavily on the heat exchange between the ocean and the atmosphere. The negative temperature feedback regulates the strength of the overturning in the following way: weak overturning leads to a reduced poleward heat transport, cold high-latitude surface temperatures, and thus enhanced density and deep water formation. With Haney restoring

boundary conditions, strong coupling to a fixed restoring temperature suppresses this important feedback. Rahmstorf and Willebrand (1995) concluded that due to the temperature feedbacks, the conveyor belt circulation is more stable than previous model studies suggested.

1.2.3 Positive feedback and multiple equilibria

Many studies of transitions between different equilibrium states have focused on salinity changes in the North Atlantic convection regions. This area is a sensitive region to the stability of the thermohaline circulation. The main reason for the nonlinear behavior of the ocean circulation is the existence of positive feedback mechanisms. We know of at least two major positive feedbacks that affect the large scale thermohaline circulation; an advective and a convective feedback.

The advective feedback refers to the mechanism whereby the thermohaline circulation advects salty water northward in the Atlantic, this enhances salinity and density in the north, which in turn maintains the thermohaline circulation (Stommel 1961; Bryan 1986b) (see Section 1.1). Due to the convective feedback, convective vertical mixing continually removes freshwater from the surface in areas of net precipitation. It thus prevents the formation of a fresh light surface layer that could stop convection (Welander 1982; Lenderink and Haarsma 1994).

Both feedbacks can reinforce an existing circulation pattern and help maintain it once initiated. This enables several different stable circulation patterns, i.e. multiple equilibrium states of the circulation are possible. Transitions between different modes of circulation can lead to major regional climate changes and can even have a global effect (see Section 1.1).

1.2.3.1 Advective spin down

The mode transition associated with the advective feedback is called an advective spin down. It has a centennial time scale and is caused by long term changes in climatic forcing, such as an increase in net precipitation or a warming of the atmosphere near a deep water formation region. The freshwater forcing increases beyond a threshold such that the circulation can no longer be maintained, and the salt advection positive feedback leads to a reversal of flow. This stability behavior can be reproduced with ocean general circulation models (Rahmstorf 1995; Rahmstorf 1996).

1.2.3.2 Convective instability

The mode transition associated with the convective feedback is called a convective instability. It is a more dramatic process, leading to circulation changes on a time scale of a decade or so. This mechanism could explain some of the abrupt climate changes seen in the ice core record, e.g., the Younger Dryas event (Weaver and Hughes 1992). There are two types of convective instability: a basin-wide event (polar halocline catastrophe; see Section 2.2) and a local one. A basin-wide convective instability interrupts all deep water formation in the ocean basin and leads to a rapid collapse of the thermohaline circulation (Bryan 1987). Welander's (1982) conceptual model demonstrates that the upper ocean is connected to the deep ocean only through convective mixing, and coupled to the atmosphere via mixed boundary conditions. In a certain range of forcing parameters, there exists a regime with two stable equilibria, one with convection and one without, depending only on initial conditions. A negative density perturbation at the surface stops convection. Once convection is off, freshwater accumulates in the surface box, reinforcing the collapsed mode. In contrast, a localized convective instability shuts down convection in one area and leads to a rearrangement of convection patterns without shutting down the large scale circulation. For example, it can cause a shift of convection from the Greenland Sea to a different location south of Iceland. Although not as dramatic as a complete shutdown of the circulation, shifts in convection pattern can also have a major effect on climate (Rahmstorf 1994).

The circulation changes discussed above could also occur as a passive response of the ocean to changes in the forcing; however, the positive oceanic feedbacks make the response highly nonlinear. These feedbacks can strongly amplify the reaction of the climate system to fairly gradual and subtle forcing changes.

1.2.4 Thermohaline variability

1.2.4.1 Millennial/centennial oscillations and mixed boundary conditions

Apart from the mode changes, the thermohaline ocean circulation can also sustain more or less regular oscillations of decadal to millennial time scale (Weaver et al. 1993; Winton and Sarachik 1993). For example, Winton and Sarachik (1993) generated millenial scale oscillations by enhancing the diagnosed equilibrium salt flux upon the switch to mixed boundary conditions. They detail the dynamics of such oscillations as well as centennial scale "loop" oscillations produced in a three-dimensional ocean model with idealized geometry and

somewhat simplified dynamics. The deep decoupling oscillation is a mode of long term variability which involves an oscillation between two near-equilibrium states, one where the thermohaline circulation is strong (the coupled phase), and one where the thermohaline circulation is weak (the decoupled phase). During the strong phase, the thermohaline circulation is gradually reduced due to the freshwater forcing. Ultimately, the high latitude conditions become such that convection breaks down, similar to a polar halocline catastrophe, and the thermohaline circulation becomes very weak. Subsequently, the deep ocean is diffusively heated over a time of order 1,000 years, until finally static instability at high latitudes occurs. Then all of the heat is released in a spectacular flush lasting for about a decade. Marotzke (1989) has also found a similar event in an ocean general circulation model with idealized geometry. The thermohaline circulation that can exceed 100 Sv (1 Sv = 10^6 m^3s^{-1}) during the flush is then reestablished, and the cycle starts again. The details of the oscillation can vary.

The deep decoupling oscillation can occur if the freshwater forcing is sufficiently strong so that the state with strong thermohaline circulation cannot reach equilibrium, but not so strong that a substantial thermohaline circulation is prevented at all times. It is not clear whether such conditions ever existed in the real climate system, but there is some evidence from the paleo-record that rapid events involving the Atlantic thermohaline circulation have actually occurred (Broecker et al. 1985) (see Section 1.1). Note that the time scales for both the convective breakdown as well as the flush are clearly decadal, although the overall period of this oscillation is millenial.

In summary, when mixed boundary conditions are used, the thermohaline circulation seems to be unstable: multiple thermohaline circulation equilibria (Stommel 1961; Bryan 1986a,b; Manabe and Stouffer 1988; Marotzke et al. 1988; Marotzke and Willebrand 1991; Quon and Ghil 1992; Marotzke 1994) and oscillations ranging from ten to thousands of years (Marotzke 1989; Mikoloajewicz and Maier-Reimer 1990; Weaver and Sarachik 1991a,b; Weaver et al. 1991; Chen 1993; Winton and Sarachik 1993; Quon and Ghil 1995; Winton 1995; Edwards et al. 1999) are found.

Oceanic variability at different spatial and temporal scales has emerged from the studies described above. Somewhat different mechanisms appear to be responsible for the oscillatory or quasi-oscillatory oceanic behavior in different modeling scenarios. Most of these studies consider the ocean alone, although attempts have been made to examine

atmosphere/ocean and sea ice/ocean interactions. The ocean-only experiments, because of their relative simplicity, should be useful for isolating the mechanism of the variability.

1.2.4.2 Decadal oscillations and mixed boundary conditions

Several studies of ocean-only models forced with mixed boundary conditions (Weaver and Sarachik 1991b; Chen and Ghil 1995; Yin and Sarachik 1995; Lenderink and Haarsma 1999) exhibit robust decadal-scale variability related to the thermohaline circulation. Weaver and Sarachik (1991b) and Yin and Sarachik (1995) associate this behavior with the location of the convection regions altering in response to the advection of salinity anomalies within the subpolar gyre. The creation and melt of sea ice can also influence the location and strength of convection regions (Zhang et al. 1995; Lenderink and Haarsma 1996) and hence play a role in the variability of the thermohaline circulation. A third type of oscillation, termed a loop oscillation by Winton and Sarachik (1993) and also discussed by Weaver et al. (1993) and by Mikolajewicz and Maier-Reimer (1990), is associated with the transport of anomalies by the meridional overturning circulation.

Weaver and Sarachik (1991b) first reported decadal variability in an ocean model forced by mixed boundary conditions. These oscillations involved substantial changes in the thermohaline circulation, with deep water formation turning on and shutting off during each cycle, and meridional heat transport changing by a factor of three. They described it as an advective, three-dimensional, high-latitude phenomenon. According to their description, a saline anomaly is first generated when warm and saline water from the separated western boundary current passes through a net evaporation region located in the mid-ocean, between the subtropical and subpolar gyres. This positive density anomaly is then advected by the mean current to the eastern boundary. During this time interval, it is convected down into the deeper ocean, leading to thermohaline circulation intensification. The intensified thermohaline circulation advects water more rapidly through the net-evaporation region and hence the surface water becomes less saline than the previous loop. The area north of the region where $E - P > 0$ and the surface water sinks is now less saline, slowing down the thermohaline circulation. The time scale was set by the advection of anomalies between the subtropical gyre and the subpolar sinking region. The existence of transient variability was found to depend on the forcing, and in particular required sufficiently strong freshwater fluxes (Weaver et al. 1993).

Lenderink and Haarsma (1999) investigated the mechanism causing a decadal oscillation in an ocean model forced by mixed boundary conditions. The oscillation is similar to the oscillation described in Winton and Sarachik (1993), Weaver et al. (1993), and Yin and Sarachik (1995). The oscillation is characterized by large fluctuations in convective activity and atmospheric heat flux in a relatively small area in the northeastern part of the basin. When the convective area is shrinking, an increasing amount of fresh water from the polar boundary of the basin is now flowing with a southward surface flow into the convective area. This causes a gradual surface freshening and eventually leads (in combination with the stabilizing effect of subsurface cooling due to the release of heat to the atmosphere) to the suppression of convection. In the absence of convection, the subsurface temperature rises due to the northward advection of warm water at the subsurface. Also the southward advection of fresh water decreases. This triggers convection again, and enables an expansion of the convective area. Thereafter the whole cycle starts again. Lenderink and Haarsma (1999) conclude that oscillations obtained with mixed boundary conditions seem to be caused by a complex interaction between temperature and salinity effects. These oscillations are commonly characterized by relatively large fluctuations in convective activity, air/sea heat flux, rapid surface salinity changes and changes in the strength of the meridional overturning rate on an (inter)decadal time scale.

Greatbatch and Peterson (1996), in agreement with Winton (1996), argued that oscillations are mainly caused by propagating waves along the boundary of the basin, and that the convective activity is due to these propagating waves. They suggested that these waves are sufficiently slowed along the weakly stratified polar boundaries, where convection take place, to give rise to decadal periods.

1.2.4.3 Fixed flux boundary conditions and decadal variability

Decadal-scale variability related to the thermohaline circulation has been shown in several studies of ocean-only models forced with fixed flux boundary conditions (Huang and Chou 1994; Greatbatch and Zhang 1995; Winton 1997; Huck et al. 1999). Several researchers have shown that fixed flux variability involves the cycling of a density anomaly (Huang and Chou 1994; Greatbatch and Zhang 1995; Chen and Ghil 1995). When a dense anomaly is in the sinking region, it accelerates the overturning, casting up a buoyant anomaly, which

subsequently retards the overturning to the point where the fixed buoyancy fluxes convert it to a dense anomaly once again.

Greatbatch and Peterson (1996), in agreement with Winton (1996), proposed an explanation for decadal oscillations based on the propagation of frictional boundary waves. They suggested that these waves are slowed along the weakly stratified polar boundaries, where convection takes place, thus giving rise to decadal periods. In contrast, Huck et al. (1999) did not find any evidence for this mechanism in their study and they suggest that a boundary wave propagation mechanism is not always appropriate. They showed that their oscillations were primarily geostrophically driven, very sensitive to damping by horizontal diffusion, and more likely to be generated by a strong circulation. In addition, the initial perturbation appeared in the regions of strongest surface cooling and the amplification of the anomalies around the western boundary was geostrophically driven.

1.3 Current research questions

1.3.1 Role of internal parameters

Several studies have performed parameter sensitivity analyses for the vertical and horizontal diffusivities (Winton and Sarachik 1993; Yin and Sarachik 1995; Huck et al. 1999). Huck et al. (1999) found horizontal temperature diffusion to be the most critical damping term for the variability. They suggested that there is a critical value of the horizontal diffusivity above which oscillations are damped out. Their study also showed that the horizontal diffusion controls the regularity of the oscillation, its amplitude, and period such that increasing the value lengthened the oscillation period and reduced the amplitude. According to Huck et al. (1999), vertical diffusion has a driving role on the variability (through its influence on the meridional overturning), while horizontal diffusion has a crucial damping role. Their study showed that interdecadal oscillations stand out as a robust geostrophic feature of thermohaline circulation models forced by constant surface fluxes in idealized geometry, but their amplitude and period is controlled by parameterized subgrid-scale diffusion processes.

Winton and Sarachik (1993) examined thermohaline circulation sensitivity to variations in the vertical diffusivity and found that increased vertical diffusivity stabilizes oscillating solutions into steady, thermally direct circulations. They found that deep decoupling oscillations appeared in both two-and three-dimensional models, but that they

occur over a much broader range of forcing in the three-dimensional model. They showed that this was due to heat and salt transports by the horizontal plane motions in the three-dimensional model that intensify in the upper polar ocean in response to the formation of a halocline and eventually destabilize it. Increasing the wind stress in the three-dimensional model stabilized oscillating solutions. In addition, their study showed that the amplitude, shape and period of the oscillations are also sensitive to the strength of the salinity forcing.

From an ocean-only model with mixed boundary conditions, Yin and Sarachik (1995) produced interdecadal oscillations that depended primarily on advective and convective processes. They found that these oscillations were not sensitive to either the detailed distribution of subpolar freshwater flux or the horizontal diffusivity. Yin and Sarachik (1995) also carried out sensitivity experiments to surface wind stress. They found that the regime of model interdecadal oscillations was sensitive to variations in wind stresses. It turned out that the model could be brought into a regime of multiple timescale oscillations superposed on each other when the magnitude of the wind stress changes. These authors suggested that the effect of wind stress is indirect: it contributes to the horizontal heat transport in the upper ocean, but it is not essential to the formation of deep water. Because wind stresses play an important role in surface fresh water and subsurface heat transports, it is not surprising that the parameter regime of interdecadal oscillations shows strong sensitivity to it. These authors plan to investigate the nature of the transition from different model parameter regimes.

1.3.2 Use of idealized salt fluxes

As reported by Greatbatch and Zhang (1995) and Huang and Chou (1994), respectively for the thermally and salinity driven circulations, zonally uniform buoyancy fluxes (varying with latitude) can induce decadal oscillations. Cai et al. (1995) added that a small zonal redistribution of surface buoyancy fluxes, diagnosed at equilibrium under restoring boundary conditions, triggers interdecadal variability.

Huck et al. (1999) showed that decadal oscillations appear spontaneously under zonally uniform constant heat flux (varying with latitude) in a large realistic range of parameters. Under diagnosed heat fluxes from the restoring runs, they observed an intensification of the variability in the western regions compared to the variability under zonally uniform averaged fluxes. Their diagnosed fluxes, also strongly intensified in the

western regions especially because of the intense cooling above the warm western boundary current, likely influenced the local stability of the circulation.

1.3.3 Influence of topography

Edwards et al. (1998) used a frictional geostrophic model to examine how the stability of the thermohaline circulation is affected by idealized topographic variations and the presence or absence of wind stress. They found that a large scale bottom slope up toward the north or the west could significantly destabilize the circulation by modifying the barotropic flow and reducing the depth of convection. The presence of an upward sloping bottom significantly reduced the stability of the solution to deep decoupling oscillations. They reported that convection and topographic forcing interact strongly and nonlinearly, and their results suggest that the westward diversion of sinking fluid and the reduced depth of convection both contribute significantly to the destabilization of the flow. In addition, they concluded that up slope leads to a significant reduction in period, while removing the wind stress also reduces the period. It appeared that wind forcing could promote destabilization by salinity advection toward the northern wall, prematurely ending the collapsed phase and reducing the oscillation period. In their study, a slope to the east did not destabilize the flow.

Winton (1997) compared the response of flat and bowl-shaped basins to fixed heat fluxes of various magnitudes, and determined that coastal topography had a considerable damping influence upon internal decadal oscillations of the thermohaline circulation. In addition to having a smaller amplitude, the bowl model produced qualitatively different oscillations than the box-shaped model. In mixed boundary condition experiments, Moore and Reason (1993) and Weaver et al. (1994) found that their models oscillated with flat bottoms but were steady when topography was included. Winton (1997) suggested that, because the mixed boundary condition models (Moore and Reason 1993; Weaver et al. 1994) exhibited the same sensitivity to topography as the fixed flux boundary condition model, a single mechanism underlies the internal decadal variabilities of both.

Yin and Sarachik (1995) performed two experiments under restoring boundary conditions: one with topography and the other without. They found that the freshwater flux diagnosed from the equilibrium with the topography is different from the freshwater flux diagnosed from the equilibrium without the topography. These authors showed that inclusion of topography can lead to an overall change in the circulation and surface freshwater flux. In

conclusion, Yin and Sarachik (1995) reported that topography does not necessarily destroy oscillations, as Moore and Reason (1993) suggested, but simply changes the freshwater flux.

1.3.4 Research focus

This thesis is presented in the following form. Chapter 2 contains a description of the ocean model and an outline of the experimental design. The following three chapters report the experiments designed to examine the influence of internal model parameters, external forcing, topography, and initial conditions on the model behavior. It is shown that ocean models have several key sensitivities that potentially lead to the instability of the thermohaline circulation. Slight alterations to the design of the numerical ocean model resulted in very different types of model behavior. This study offers an important perspective concerning the validity of ocean modeling studies by examining how typical methodologies can produce widely divergent behavior. Chapter 3 reports the experiments that examined the influence of internal parameters on the flow characteristics and oscillatory behavior of the model. This section verifies the significance of internal parameters in determining the resulting ocean circulation. Chapter 4 presents the results from the experiments that analyzed the impact of surface boundary conditions on the thermohaline circulation. It is shown that the zonal variability of the salinity fluxes is critical in maintaining a steady overturning circulation. Chapter 5 describes the experiments conducted with different idealized topographies. These experiments showed the wide range of behavior that is possible when two dimensional diagnosed salinity fluxes are used with varying topographies. The conclusions are presented in Chapter 6.

2. Model description and experiments

2.1 Description

2.1.1 Governing equations

Three-dimensional ocean general circulation models are useful tools for process studies of the role of the ocean, and in particular its thermohaline component, in future and past climate change and variability. The primitive equation model used in this study is the well-tested and widely used Bryan-Cox ocean general circulation model based on the pioneering work of Bryan (1969) and described by Cox (1984) and Pacanowski et al. (1991). The notation used is standard.

The equations that govern the oceanic flow in this model are the horizontal and vertical momentum balance, conservation of heat and salt, mass continuity, and the equation of state. Several simplifying assumptions are made based on our understanding of the nature of large scale oceanic flow. Two assumptions are made in the momentum equations:

1) The hydrostatic approximation is used in which all terms of the vertical momentum balance are neglected except gravity and the vertical pressure gradient force. This allows vertical motion to be a diagnostic variable rather than a prognostic variable;

2) The Boussinesq approximation is applied so that small variations of density are neglected in the horizontal pressure gradient term. This assumption both simplifies the momentum equations and also filters out sound waves that are unimportant to the oceanic flow. In assuming non-divergence of the oceanic flow mass, continuity is simplified and vertical motion can be calculated diagnostically.

The numerical methods applied to solve the governing equations use a finite grid of points. The processes that occur on scales below the resolution of the model grid need to be parameterized. Eddy viscosities and diffusivities are typically used (see Section 2.1.4).

The seven governing equations in seven variables are cast in spherical coordinates (ϕ, λ, z) where ϕ is the latitude, λ the longitude, and z the depth. The variables are zonal, meridional and vertical velocity (u, v, w), temperature (T), salinity (S), pressure (p), and density (ρ). The equations below are taken from Semtner (1986):

$$\frac{\partial u}{\partial t} + M(u) - fv = \frac{-1}{\rho_0 a \cos\phi}\frac{\partial p}{\partial \lambda} + A_{MV}\frac{\partial^2 u}{\partial z^2} + A_{MH}\left(\nabla^2 u + \frac{(1-\tan^2\phi)u}{a^2} + \frac{2\sin\phi}{a^2\cos^2\phi}\frac{\partial v}{\partial \lambda}\right) \quad (2.1)$$

17

$$\frac{\partial v}{\partial t} + M(v) + fu = \frac{-1}{\rho_0 a}\frac{\partial p}{\partial \phi} + A_{MV}\frac{\partial^2 v}{\partial z^2} + A_{MH}\left(\nabla^2 v + \frac{(1-\tan^2\phi)v}{a^2} + \frac{2\sin\phi}{a^2\cos^2\phi}\frac{\partial u}{\partial \lambda}\right) \quad (2.2)$$

$$\frac{\partial p}{\partial z} = -\rho g \quad (2.3)$$

$$\frac{1}{a\cos\phi}\frac{\partial u}{\partial \lambda} + \frac{1}{a\cos\phi}\frac{\partial(v\cos\phi)}{\partial \phi} + \frac{\partial w}{\partial z} = 0 \quad (2.4)$$

$$\frac{\partial T}{\partial t} + M(T) = A_{DV}\frac{\partial^2 T}{\partial z^2} + A_{DH}\nabla^2 T \quad (2.5)$$

$$\frac{\partial S}{\partial t} + M(S) = A_{DV}\frac{\partial^2 S}{\partial z^2} + A_{DH}\nabla^2 S \quad (2.6)$$

$$\rho = \rho(T,S,p) \quad (2.7)$$

Where,

$$M(\alpha) = \frac{1}{a\cos\phi}\frac{\partial(u\alpha)}{\partial \lambda} + \frac{1}{a\cos\phi}\frac{\partial(v\alpha\cos\phi)}{\partial \phi} + \frac{\partial(w\alpha)}{\partial z} \quad (2.8)$$

$$\nabla^2 \alpha = \frac{1}{a^2 \cos^2 \phi} \frac{\partial^2 \alpha}{\partial \lambda^2} + \frac{1}{a^2 \cos^2 \phi} \frac{\partial(\partial \alpha \cos \alpha / \partial \phi)}{\partial \phi}$$ (2.9)

And the Coriolis parameter,

$$f = 2\Omega \sin \phi$$ (2.10)

A_{MV}, A_{MH}, A_{DV}, and A_{DH} are the coefficients of vertical and horizontal eddy viscosities and vertical and horizontal eddy diffusivities respectively (described below).

The equation of state (Eq. 2.7; Pond and Pickard 1983) is a nonlinear function of temperature, salinity and pressure. Bryan and Cox (1972) have developed a polynomial expansion of this equation suitable for modeling. In this study, intense vertical diffusion of temperature and salinity homogenizes the column when it becomes unstable (Cox 1984). This process is performed implicitly and does not require further iterations. An enhanced value of the vertical eddy diffusivity (A_{DV}) is used for convective adjustment and its value in this set of experiments is 10^4 cm^2/s. This value is four orders of magnitude larger than the typical value for A_{DV}.

2.1.2 Boundary conditions

In this model the only source of heat and salinity forcing is at the upper surface. A no-flux condition is imposed at the side-walls and bottom. There is a no-slip (u,v=0) condition for the vertical side walls. At the bottom boundary, the flow is constrained to be parallel to the bottom topography. For the initial series of experiments, the model has a flat bottom, and w=0 at the bottom. The imposed bottom friction determines the condition on u and v,

$$\tau_\lambda = \rho_0 C_D (u^2 + v^2)(u \cos \alpha - v \sin \alpha)$$ (2.11)

$$\tau_\phi = \rho_0 C_D (u^2 + v^2)(u \sin \alpha - v \cos \alpha)$$ (2.12)

where C_D, the drag coefficient, is 1.3 x 10^{-3} and α, the turning angle, is -10^0 for this study.

The rigid lid approximation (w=0 at z=0) is used as the upper boundary condition for the vertical velocity. This condition filters out high frequency surface gravity inertia waves and thus allows a larger time step for the model. The atmospheric winds force the horizontal momentum at the upper surface. This is diagnosed by using wind stresses $(\tau_\lambda, \tau_\phi)$ from observation of the atmosphere or by using an analytic function to approximate them. The second approach was taken for this study such that surface winds are prescribed by the following analytic representation,

$$\tau_\phi = 0.2 - 0.8\sin(6\phi)$$

(2.13)

$$\tau_\lambda = 0.0$$

(2.14)

where the wind stress is in units of dynes/cm^2. This choice is designed to give a two-gyre circulation in the North Atlantic as this is the approximate region of the model domain.

There are two common approaches to the parameterization of the upper boundary condition for temperature and salinity: 1) restoring temperatures and salinities to prescribed values; and, 2) prescribed heat and salt fluxes. Haney (1971) developed the technique of restoring boundary conditions on temperature for parameterizing the heat flux. Heat exchange at the ocean surface depends on the downward solar radiation, the upward flux of longwave radiation, sensible heat flux, and the latent heat flux. These contributions were linearized and presented by Haney (1971) in the following form,

$$H = D\left(T^* - T^S\right)$$

(2.15)

where H is the heat flux into the ocean and T^S is the ocean surface temperature. The effective temperature T^* includes the contribution of latent and sensible heating. The diffusion constant, D, is empirically derived using climatological data of surface vapor pressure, wind speed, cloud cover, and transfer coefficients. In general, T^* and D vary spatially and temporally (Yuen et al. 1991). The variation of D is small and T^* is not significantly different from the atmospheric temperature at the ocean surface away from the equator and poles.

A restoring boundary condition for the salinity flux is not justified by any physical mechanism. This method implies that the salinity field is forced by the difference between evaporation and precipitation. Although the surface temperature of the ocean directly affects the heat flux, the freshwater flux is not driven by a similar feedback. Evaporation and precipitation are independent of the surface salinity and evaporation is a function of temperature. It is the ease of implementing a restoring boundary condition on the salinity flux and its guarantee of simulating prescribed conditions that has led to its widespread use in ocean general circulation models.

Restoring boundary conditions are typically used until an equilibrium state has been achieved. The salt flux is then diagnosed and used for further integration of the model ocean. The stability of the equilibrium to the new mixed surface boundary condition has been the subject of considerable interest (Lenderink and Haarsma 1999; Edwards et al. 1998; Chen and Ghil 1995; Winton and Sarachik 1993; Weaver and Sarachik 1991a,b; Marotzke 1991).

In this work restoring boundary conditions are used for both temperature and salinity (Haney 1971) during the initial spin up phase. The restoring values are taken from the Levitus (1982) data set. Both the restoring temperatures and salinities are functions of latitude only and do not vary temporally. The diffusion constant, D, is constant spatially and temporally, and corresponds to a restoring time scale of 50 days for a 50 m upper layer. More detailed descriptions of the model configuration and boundary conditions can be found in several other studies (Gough 1991; Gough and Lin 1992; Gough and Welch 1994).

2.1.3 Numerics

Given the assumptions mentioned above, the seven dependent variables are reduced to four prognostic variables: the two components of horizontal motion, temperature and salinity. Vertical motion is diagnostically calculated through the mass continuity equation (Eq. 2.4). The equation of state is used to calculate density (Eq. 2.7).

Calculations were performed for an Arakawa B grid (Arakawa 1966) which is used for its energy and conservation properties. Temperature and salinity are evaluated on one grid while the horizontal velocities are evaluated on another grid displaced half a grid interval in both horizontal directions. Vertical velocity is calculated at both sets of grid points half a level above and below the horizontal grids.

The uniform grid spacing is 2^0 latitude by 2^0 longitude, and covers a domain from 20^0 - 70^0N, 0^0 - 60^0W of the North Atlantic. There are ten vertical levels, listed in (Gough and Lin 1992). These vertical layers increase with depth permitting higher resolution in the more active thermocline region.

All equations use leap frog finite differences that are centered in time, except for the Coriolis term that is treated semi-implicitly and the diffusive terms that are evaluated using values from the previous time step. This method of evaluation of the Coriolis term enables a larger time step to be used. The technique chosen for the diffusive terms ensures numerical stability. A forward time step is performed every 20 steps to suppress the growth of the computational mode in the leap frog scheme. There are several numerical constraints on the time step and on the eddy viscosities and eddy diffusivities due to the type of grid and the numerical schemes used (Bryan et al. 1975).

2.1.4 Parameterization in ocean models

Coarse resolution models ($>1^0$) are dependent on tunable parameters used to approximate sub-grid scale processes. These models are not capable of resolving mesoscale eddies, salt fingering, double diffusion, internal breaking waves, and convection. Mesoscale eddies mix laterally and have traditionally been represented by horizontal diffusion. The vertical mixing of temperature, salt and other ocean tracers is caused by salt fingering, double diffusion and internal breaking waves. This has been represented as vertical or diapycnal diffusion (perpendicular to lines of constant density). Eddy diffusivities are used in the temperature and salinity equations (Eq. 2.5 and Eq. 2.6, respectively). The horizontal diffusivity coefficient is typically seven orders of magnitude larger than the vertical diffusivity; however, the model flow is very sensitive to the vertical diffusivity. Bryan (1987) found that the depth of the thermocline, the meridional and zonal mass transport and the northward heat transport among other quantities depended on the value chosen for the eddy diffusivity. Gough and Allakhverdova (1998) found modest variations of these eddy diffusivity coefficients produced more of an impact than typical warming or cooling scenarios.

2.2 Overview of experiments

In this work, the stability and variability properties of the thermohaline circulation were studied using a one-basin, coarse-resolution ocean numerical model. Qualitative and quantitative characteristics of simulations generated with the three dimensional ocean model were examined by varying internal parameters, surface boundary conditions and changes in topography.

For the initial experiments, statistical techniques (Gough and Welch 1994) were used to design computer simulations to explore a five input parameter space of an ocean model. By simply changing the tunable model inputs, widely divergent model behavior was produced. These experiments were also conducted using mixed boundary conditions with isohaline and isothermal initial conditions. Compared to the models that were integrated with the steady state obtained at the end of the spin up, there were no qualitative and only minor quantitative differences in the resulting ocean circulation. This test of the impact of the initial conditions in determining model behavior showed that initial conditions are the least important of the factors considered in effecting the thermohaline circulation.

In subsequent experiments, the initial simulations were run with new temperature and salinity restoring boundary conditions. The values for the original boundary condition were selected from the Levitus (1982) data set. The new experiments used restoring boundary conditions with a sine distribution of temperature and salinity. The impact on the ocean model behavior of changing the surface boundary conditions was examined. In addition, all cases were run with both two dimensional salinity fluxes and zonally averaged salinity fluxes. This allowed a comparison of the influence of salinity forcing on the oscillatory behavior of the thermohaline circulation.

A third series of experiments examined the influence of ocean basin topography on the model's oscillatory circulation. The original flat-bottom ocean was modified to produce five new scenarios: a) north sloping; b) west sloping; c) south sloping; d) east sloping; and e) bowl-shaped (north, west and east sloping). This analysis investigated whether more realistic bottom topography would stabilize the behavior of the thermohaline circulation.

2.2.1 Equilibrium simulations

Beginning at an initial state of rest, all simulations were integrated to two thousand years. A split time step method was used (Bryan 1984). The temperature and salinity

equations employed a two day time step whereas the momentum equations used a thirty minute time step. Due to the nature of the restoring field for the Levitus and sine restoring boundary conditions, a density driven circulation arose. Typically, there was downwelling in the north where the restoring density peaked and gradual upwelling throughout much of the remainder of the domain. A wind driven Ekman circulation was also generated in the upper ocean.

2.2.2 Oscillation experiments

In order to generate oscillations, a methodology similar to Winton and Sarachik (1993) and Edwards et al. (1998) was employed involving the magnification of the surface salt fluxes. Salt fluxes were diagnosed at the end of the equilibrium simulations. For each of the cases, the salinity flux was magnified by 1.5 and integrated for at least two thousand additional years.

3. Impact of internal parameters on the flow characteristics and oscillatory behavior of an ocean general circulation model

3.1 Introduction

Coarse resolution ocean general circulation models are commonly used in process studies of the ocean circulation and climate change scenario simulations (Kattenberg et al. 1996). These models are dependent on internal parameters used to approximate sub-grid scale processes. The general purpose of this study is to further our understanding of the sensitivity of a widely used ocean general circulation model (for model description see Chapter 2) to tunable parameter values. Twenty six experiments were designed, each having a unique combination of the internal parameter values, and integrated for several thousand years while the surface boundary conditions were held constant. These model simulations were used to perform two analyses: 1) the parameter space of the ocean general circulation model was explored and compared to previously published results; and, 2) the oscillatory behavior of the model was examined under enhanced salt flux conditions. The examination of the dependency of model outputs on inputs reproduced known sensitivities of familiar flow field measures.

3.2 Methodology

In these experiments, a five input parameter space was thoroughly explored using twenty six experiments using the model described in Chapter 2. These five input parameters are the vertical and horizontal eddy diffusivities (A_{DV}, A_{DH}), the vertical and horizontal eddy viscosities (A_{MV}, A_{MH}), and the peak value of the wind stress (τ_m). The peak wind stress is varied by changing the coefficient of the sine term in Eq. 2.13 (in Chapter 2). The purpose of these experiments was to determine the dependency of model outputs on the inputs (listed in Table 3.1). The methodology used was standard (see Chapter 2, Section 2.3.1 and 2.3.2).

To ensure the efficient use of computing resources, statistical techniques were employed to design the experiments and evaluate the model output (described below, Section 3.2.2).

Table 3.1. List of model inputs and outputs

Model inputs:	Model outputs:
Vertical and horizontal eddy diffusivities (A_{DV}, A_{DH})	Kinetic energy density (KE)
Vertical and horizontal eddy viscosities (A_{MV}, A_{MH})	Peak value of the meridional overturning streamfunction MMT)
Peak value of the wind stress (τ_m)	Northward heat transport (NHT)
	Number of convectively unstable points (CONV)
	Lowest temperature at the bottom level (TBOT)
	Salt flux strength (FS)

3.2.1 Experimental design

A total of twenty six experiments (listed in Table 3.2) was performed to explore the parameter space defined by the ranges in Table 3.3. The range for each input parameter is covered by a grid with spacings of 1/25 of the range. For example, the twenty six runs for A_{DV} ranged from 0.25, 1.04, ..., 20.0. Each of these twenty six values appeared in one of the runs, but not necessarily in that order. To sample the five parameter input space uniformly, a Latin hypercube (LH) experimental design (McKay et al. 1979) was used. Within the class of LH designs, combinations of the five parameters were chosen by numerically optimizing a maximum design criterion (Johnson et al. 1990). This criterion chooses the combinations such that the design points are spread apart. Figure 3.1 shows the design combinations for A_{DV} and A_{DH}. It can be seen that the points are well spaced in two dimensions. The parameter combinations for all five inputs are listed in Table 3.2 for the twenty six experiments. In a more traditional approach one of the input parameters would be varied while the other four are held constant. If each of the five values were sampled by using three values, it would take 3^5 (or 243) simulations. The twenty six run design actually used reduces computation by an order of magnitude. Moreover, spacing each input at twenty six levels rather than three allows the possibility of detecting highly nonlinear input-output relationships.

Two of the original twenty six simulations failed to reach a steady equilibrium. These two runs, #5 and #26, had the lowest values of horizontal eddy diffusivity (0.296×10^7 cm^2/s and 0.100×10^7 cm^2/s, respectively). These results are consistent with Gough and Welch (1994), where unstable behavior was detected for runs with low horizontal diffusivity.

Table 3.2. List of experiments

Run	Vertical diffusivity (A_{DV}; cm²/s)	Horizontal diffusivity (A_{DH}; 10^7 cm²/s)	Vertical viscosity (A_{MV}; cm²/s)	Horizontal viscosity (A_{MH}; 10^9 cm²/s)	Wind stress (τ_m)
1	4.99	2.648	20.00	3.86	1.584
2	11.31	4.608	12.89	4.24	1.800
3	1.83	1.080	13.68	1.58	0.684
4	1.04	1.864	9.73	2.34	1.728
5	13.68	0.296	15.26	2.15	0.072
6	19.21	1.472	5.78	0.25	1.152
7	16.84	5.000	8.94	3.48	0.576
8	4.20	4.412	4.99	1.96	1.368
9	3.41	2.256	16.05	0.44	0.432
10	12.10	1.276	17.63	2.91	1.440
11	10.52	3.236	0.25	1.77	0.504
12	12.89	3.824	7.86	0.82	0.720
13	8.94	0.492	8.15	4.81	1.512
14	0.25	2.844	6.57	3.10	0.144
15	2.62	3.628	2.62	4.62	0.000
16	17.63	0.844	1.83	1.01	1.656
17	18.42	3.040	16.84	4.43	0.792
18	8.15	4.804	18.42	1.20	0.216
19	9.73	2.060	3.41	3.29	0.936
20	6.57	0.688	4.20	2.53	0.648
21	15.26	2.452	11.31	1.39	1.296
22	14.47	1.668	1.04	4.05	0.288
23	20.00	4.020	12.10	2.72	0.360
24	16.05	4.216	19.21	5.00	1.080
25	7.36	3.432	14.47	3.67	1.224
26	5.78	0.100	10.52	0.63	1.008
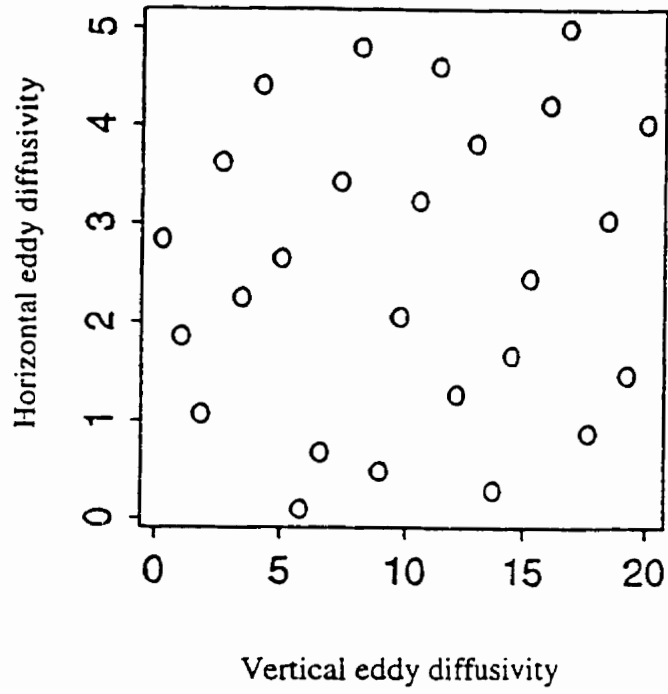
Figure 3.1. Experimental design combinations of A_{DV} and A_{DH}.

Table 3.3. Input parameter ranges

Input	Input symbol	Minimum	Revised minimum	Maximum
Vertical eddy diffusivity (cm²/s)	A_{DV}	0.25	1.04	20.00
Horizontal eddy diffusivity (10⁷cm²/s)	A_{DH}	0.1	0.394	5.00
Vertical eddy viscosity (cm²/s)	A_{MV}	0.25		20.00
Horizontal eddy viscosity (10⁹cm²/s)	A_{MH}	0.25	0.44	5.00
Peak wind stress (dynes/cm²/s)	τ_m	0.0		1.8

3.2.2 Statistical model fitting

The output data from the twenty four simulations that reached an equilibrium were modeled using an approach described in Sacks et al. (1989) and Welch et al. (1992) and used by Gough and Welch (1994). Details may be found in these references.

To describe the method briefly, let y denote one of the outputs. It is a function of the five inputs, $x = (x_1, ..., x_5)$. Then, $y(x)$ is modeled as if it were the realization of a stochastic process,

$$Y(x) = \beta_0 + Z(x) \tag{3.1}$$

Here β_0 is the mean of Y, and $Z(x)$ has mean 0 and correlation function $R(x, x')$ for the correlation between the two Z's at input vectors x and x'.

The correlation function R is critical to this modeling strategy. For many applications, the function

$$R(x, x') = \prod_l \exp\left(-\theta_l |x_l - x_l|^{p_l}\right) \tag{3.2}$$

has led to accurate prediction. The unknown parameters, θ_l and p_l are estimated by maximum likelihood estimation. Model (Eq. 3.1) leads to the best linear unbiased predictor (BLUP) of $y(x)$ at an untried input vector x,

$$\hat{y}(x) = \beta_0 + r^T R_D^{-1}(y - \beta_0 1) \tag{3.3}$$

where r is an $n \times 1$ vector of correlations with element i given by $R(x, x_i)$ from (Eq. 3.2), y is the $n \times 1$ vector of output values from the numerical model for a particular response, and x_i is for run i in the experiment, R_D is an $n \times n$ matrix of correlations between Z's at the design points with i, j given by $R(x, x_i)$ from (Eq. 3.2), l is an $n \times 1$ vector of l's, and $\beta_0 = 1^T R_D^{-1} y / 1^T R_D^{-1} 1$ is the generalized least squares estimator of β_0.

In contrast to regression models, this predictor is able to model nonlinear relationships without explicitly specifying the form of the nonlinearity. Similarly, interaction effects between two or more input parameters need not be specifically modeled. The data identify complex features of the relationship automatically.

Once the model is fitted, the input-output relationship can be explored via the BLUP (Eq. 3.3) without generating new simulations. For reliable exploration, however, the BLUP should provide accurate prediction. Prediction accuracy is often assessed via leave-one-out cross validation. The output $y(x_i)$ for simulation I is predicted from the BLUP (Eq. 3.3) built from all data except run i, denoted by $y_{-i}(x_i)$ to emphasize that run i is removed when computing y. Comparison of $y(x_i)$ and $y_{-i}(x_i)$ values for each output gives an indication of the reliability of the statistical methods.

By first looking at familiar measures of the model flow, statistical approximating functions were used to represent the ocean model. They were then used to estimate the importance of the various inputs on the value of several zero dimensional outputs. The exceptionally large kinetic energy values are somewhat underpredicted. Otherwise, the ocean general circulation model is reasonably predictable, and subsequent results and inferences about sensitivities appear to be based on reliable approximations.

The statistical approximating functions reproduced known model sensitivities. For example, scaling relationships between the vertical eddy diffusivity and the meridional overturning streamfunction, the northward heat transport, and the zonal overturning streamfunction were produced within the values reported in the literature (Bryan 1987; Colin de Verdiere 1988; Bryan 1991; Winton 1996; Gough and Allakhverdova 1998). In addition, the dependence of the overturning streamfunction on the horizontal eddy diffusivity was examined. Cross validation analysis showed that the statistical approximating functions performed well.

3.3 Results and Discussion

3.3.1 Dependencies of output on input – flow field measures

One of the main purposes of these experiments was to examine the parameter space of a well distributed ocean general circulation model. Two of the original twenty six simulations failed to reach a steady equilibrium. These two runs, #5 and #26, had the lowest values of horizontal eddy diffusivity (0.296×10^7 cm^2/s and 0.100×10^7 cm^2/s, respectively). Previous studies have also shown that unstable behavior occurs for runs with low horizontal diffusivity (Gough and Welch 1994).

3.3.1.1 Flow field measures

i)   Kinetic energy density (KE)

Figure 3.2 shows the main effects for the input variables estimated to have an important effect on the kinetic energy density. The main effect of the vertical diffusivity on the kinetic energy density in Figure 3.2a, for instance, is obtained by integrating the predictor with respect to the other four inputs over the revised ranges in Table 3.3, refer to Gough and Welch (1994) for details. The error bars around each plotted point give an approximate 95% confidence interval for the integral to visually allow for statistical prediction uncertainty. The percentage of 48.4% given in Fig. 3.2a shows that the main effect of the vertical diffusivity accounts for 48.4% of the total variability in the kinetic energy density predictor over the five inputs. Only inputs accounting for at least 2.5% of the variability are deemed important and displayed. There are four such inputs for the kinetic energy density. Kinetic energy density increases with increasing vertical eddy diffusivity and peak wind stress. It decreases with horizontal diffusivity and horizontal viscosity.

These sensitivities are similar to those found in Gough and Welch (1994) and are attributable to the two main circulations, wind driven and buoyancy driven. Bryan (1987) found that increasing the vertical eddy diffusivity increased the overturning streamfunction, a measure of the thermohaline circulation. Increasing the wind stress increases the Ekman circulation. Both the horizontal eddy diffusivity and viscosity act to dampen the flow (particularly the gyre component) and thus cause a reduction in the kinetic energy density.
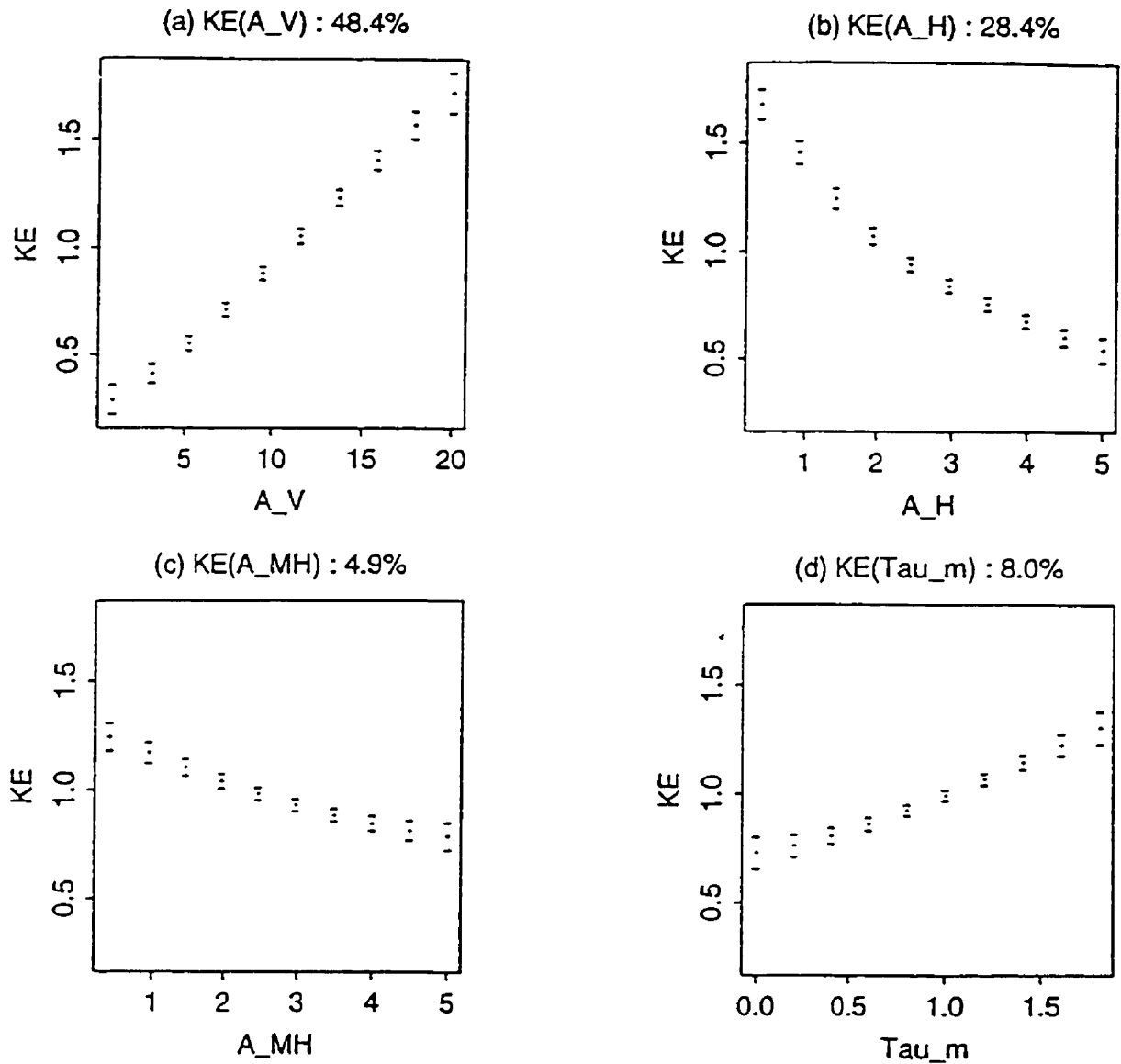
Figure 3.2 Estimated main effects for kinetic energy density (KE): (a) vertical eddy diffusivity (A_V); (b) horizontal eddy diffusivity (A_H); (c) horizontal eddy viscosity (A_MH); and (d) peak wind stress (Tau_m)

ii)   Meridional overturning streamfunction (MMT)

Fig 3.3 shows that the vertical eddy diffusivity is the dominant component in determining the peak value of the overturning streamfunction (94.5%). The horizontal eddy diffusivity plays a much smaller role.

The dependency of the vertical diffusivity is consistent with Bryan (1987) and Winton (1996). Bryan found that the overturning streamfunction had a $Av^{1/3}$ dependence, differing from a $Av^{2/3}$ dependence expected from scaling. A log-log analysis of the current results showed a dependence ranging from 1/3 for low vertical diffusivity to 1/2 for larger vertical diffusivity values.

iii)   Northward heat transport (NHT)

In Figure 3.4, it is shown that there is one dominant input, the vertical eddy diffusivity. A log-log analysis reveals a power relationship of 1/2, less than the expected 2/3 (Bryan 1991; Winton 1996) but consistent with Colin de Verdiere (1988). The Winton results had a power relationship slightly in excess of 1/2.

iv)   Number of convective points (CONV)

The number of convective points was introduced in a Gough and Welch (1994) study as a measure of the isopycnal nature of the model. A minimum in the number of convective points corresponded to the largest value of the maximum allowable isopycnal slope. For the present set of experiments, there were two important inputs, the dominant one being the vertical eddy diffusivity, while the peak wind stress played a less important role.

A larger vertical eddy diffusivity enhanced the meridional overturning (see above). This brings more warm, salty water to the northern regions. In the presence of restoring boundary conditions, this results in statically unstable conditions at the surface resulting in wider spread convection. Similarly a large wind stress transports more warm and salty water to the north.

v)   Bottom temperature (TBOT)

In the Gough and Welch (1994) study, bottom temperature was obtained at a fixed location. In this analysis the minimum temperature at the bottom level was recorded,

(a) MMT(A_V) : 94.5%

(b) MMT(A_H) : 3.2%

Figure 3.3. Estimated main effects for meridional overturning streamfunction (MMT): (a) vertical eddy diffusivity (A_V) and (b) horizontal eddy diffusivity (A_H).

NHT(A_V) : 97.7%

Figure 3.4. Estimated main effect of vertical eddy diffusivity (A_V) on northward heat transfer (NHT).
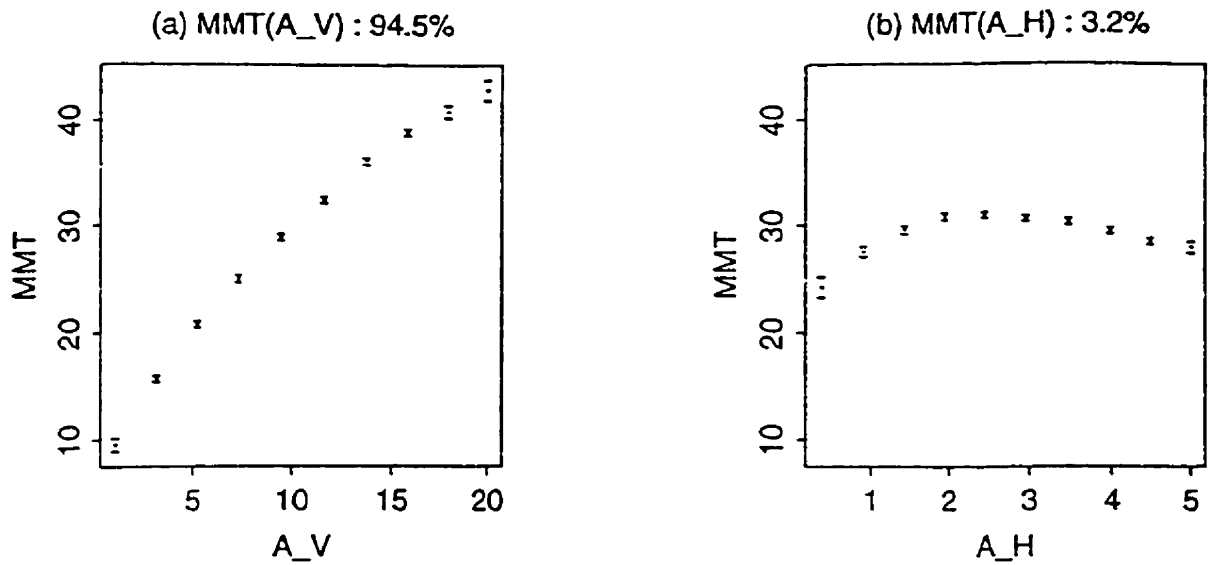
regardless of horizontal location. There are two significant inputs roughly of the same importance, the vertical eddy diffusivity and the horizontal eddy diffusivity.

The role of the vertical eddy diffusivity is readily explainable (Gough and Welch 1994). Water mass is transported via the thermohaline circulation. If this circulation is intense than the downwelling waters are not cooled as much at the surface as it is in weaker flow. The thermohaline circulation has a strong dependence on the vertical eddy diffusivity, therefore the expectation is that the bottom water temperature should increase with increasing vertical diffusivity.

There is also a dependence on the horizontal eddy diffusivity. In Gough and Welch (1994), this dependence was attributed to the mitigating effect of mixing, smoothing out extrema. In all cases, the coldest waters in the domain occur in the northeast corner of the domain at the top level. The coldest water at the bottom is typically two degrees warmer. Cold water at the surface advects and convects to lower levels and warms due to vertical and horizontal mixing and advection. Larger horizontal diffusivity values would cause warmer surface waters, as well as producing a larger heat flux, since the water sinks to the bottom. A contributing factor is the impact of the horizontal diffusivity on the flow and therefore the advective component. Increasing the horizontal diffusivity does affect the meridional overturning streamfunction although the relationship is somewhat ambiguous.

3.3.2 Oscillatory behavior under enhanced salt flux forcing

The second step of this analysis was to examine model behavior under enhanced salt flux forcing. From the remaining twenty four experiments, four behavior types were found upon switching to the enhanced salt flux surface boundary conditions. The range of behavior was categorized as explosive (E; i.e., unstable), steady state (S), high frequency oscillations (HFO), and long period oscillations (O). Three cases (#2, 8, and 15) exhibited E behavior. Two of the E cases (#2 and 15) have extreme values of the wind stress. Four cases (#4, 10, 19, and 22) after one or two thermohaline collapses, settled to S behavior. Three cases (#13, 16, and 20) exhibited HFO of decadal-centennial time scale. HFO cases produced oscillations in the upper levels of the ocean model and only caused minor changes in the bottom temperature. In comparison, O cases showed oscillations of the bottom temperature that were synchronous with the other diagnostics. Twelve cases produced O ranging in period from 340 to 2655 years.

An example of each type of response (with the exception of the explosive cases) is shown in Figure 3.5. The first diagnostics shown in these time series are the average temperature of the top five model levels (TempUp) and the average temperature of the bottom five model levels (TempDw). The other diagnostics are the number of convection points (Conv) and the kinetic energy density (KE). The examples include case #19 (S), 7 (O), and 16 (HFO).

The steady cases exhibit strong thermally direct circulations. The steady overturning circulation is characterized by convection in the polar region and a deep thermocline depth. The S cases all had horizontal diffusivity values within the range typically used with this model ($1 - 2 \times 10^7 \, cm^2/s$).

The O cases exhibit the flush/collapse cycle reported in Winton and Sarachik (1993) (see Chapter 1, Section 2.4.1) also termed deep decoupling oscillations. A diagnostic representing the strength of the salt flux (FS) was used to understand what determines the nature of the varied oscillations. The surface salt flux for case #19 (S) is shown as Figure 3.6. The largest freshwater flux occurs in the mid-latitudes near the western boundary. This peak value is used as a diagnostic representing the strength of the salt flux. Table 3.4 is a list of cases ordered according to the strength of this diagnostic. In addition, the period and type of model behavior are listed.

The E cases occur when the FS diagnostic is small whereas the HFO and S cases occur for large FS values. The O cases cover the middle range of FS values. Statistical approximating functions were developed to determine the dependency of the salt flux on the input parameters. Figure 3.7 shows the importance of the various inputs. The horizontal diffusivity dominates (70.3%), followed by the vertical diffusivity (20.6%) and wind stress (7.3%). The viscosities were not important for this diagnostic.

The HFO cases have the lowest horizontal diffusivity (A_{DH}). The low A_{DH} allows for a highly structured salt flux field. This can lead to localized oscillations such as those found by Weaver et al. (1991). The S cases tend to have higher values of A_{DH} than the HFO cases. The four S cases all fell with the range typically used with this model. It is likely that the stronger A_{DH} smooths the surface fluxes sufficiently that the high frequency oscillations are suppressed. This is consistent with Huck et al. (1999) who observe that horizontal tracer diffusion appears to be the most critical damping term for the variability. These authors report that whatever the model, the forcing conditions, or the initial state, there is a critical value of

(a)
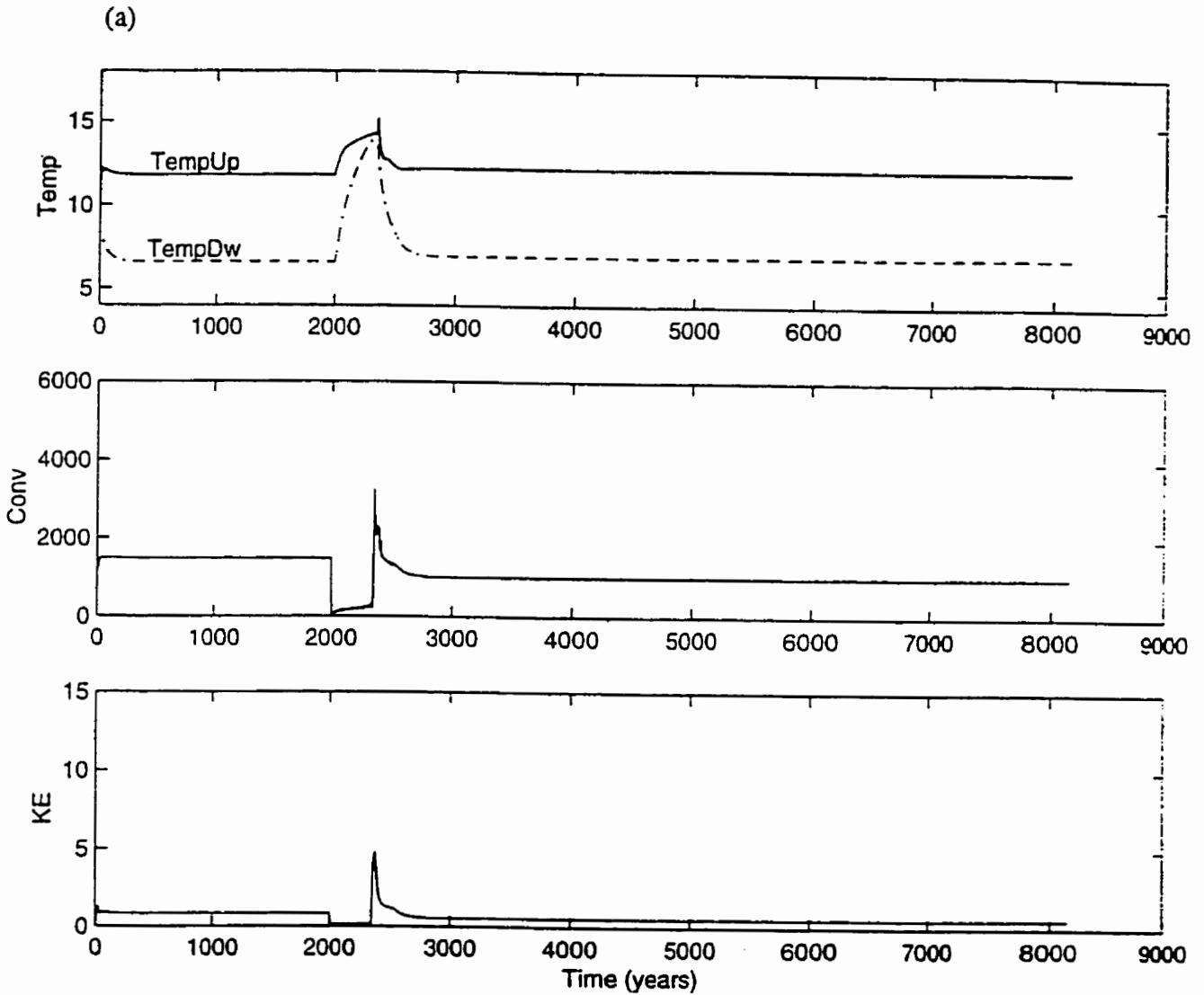
Figure 3.5 Examples of model behavior: (a) steady; (b) long period oscillation; and, (c) high frequency oscillation. The diagnostics shown are the average temperature of the top five model levels (TempUp), average temperature of the bottom five model levels (TempDw), number of convection points (Conv), and the kinetic energy density (KE). The temperature diagnostics are in units of Celsius and the other measures of model flow are zero dimensional

(b)
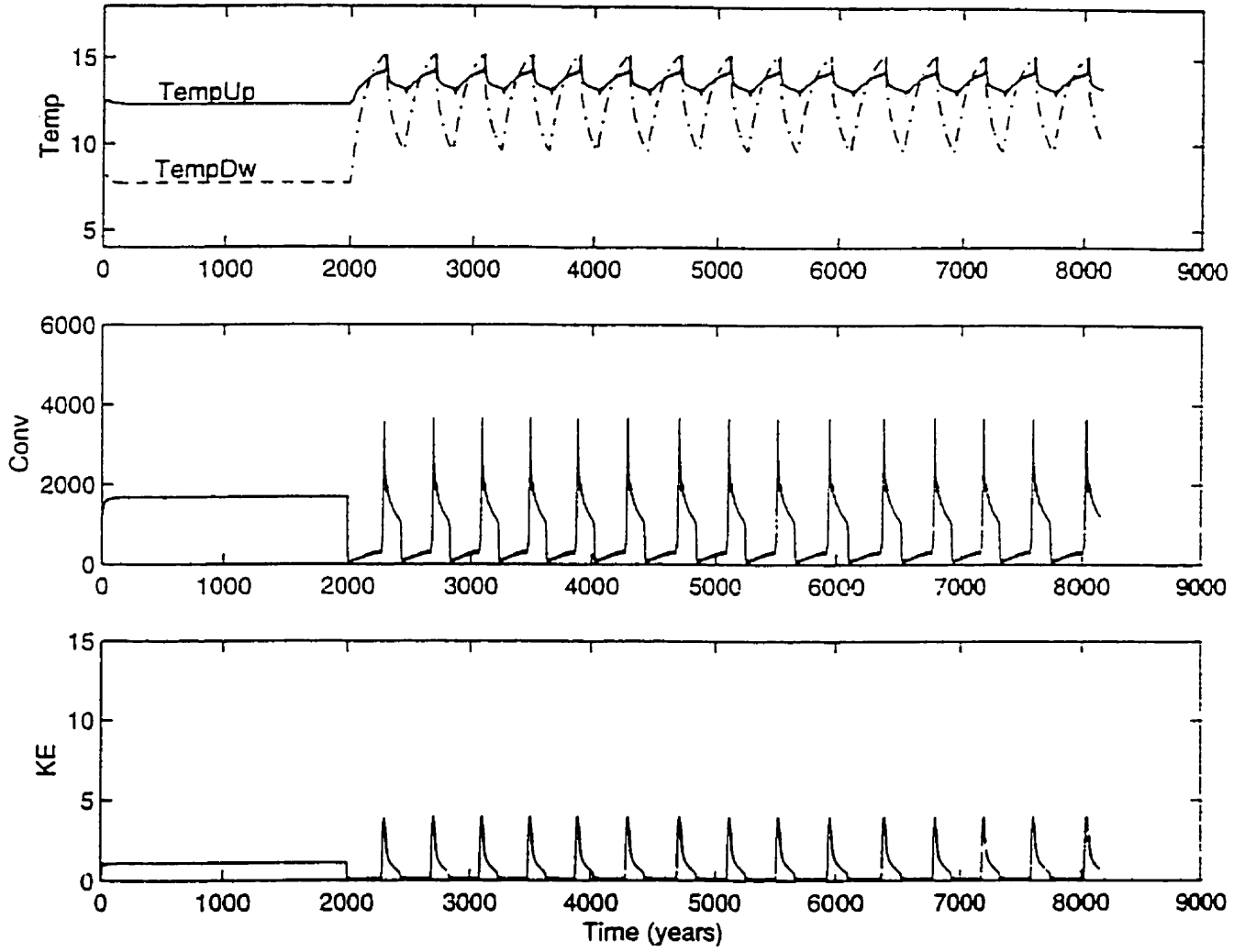
(c)
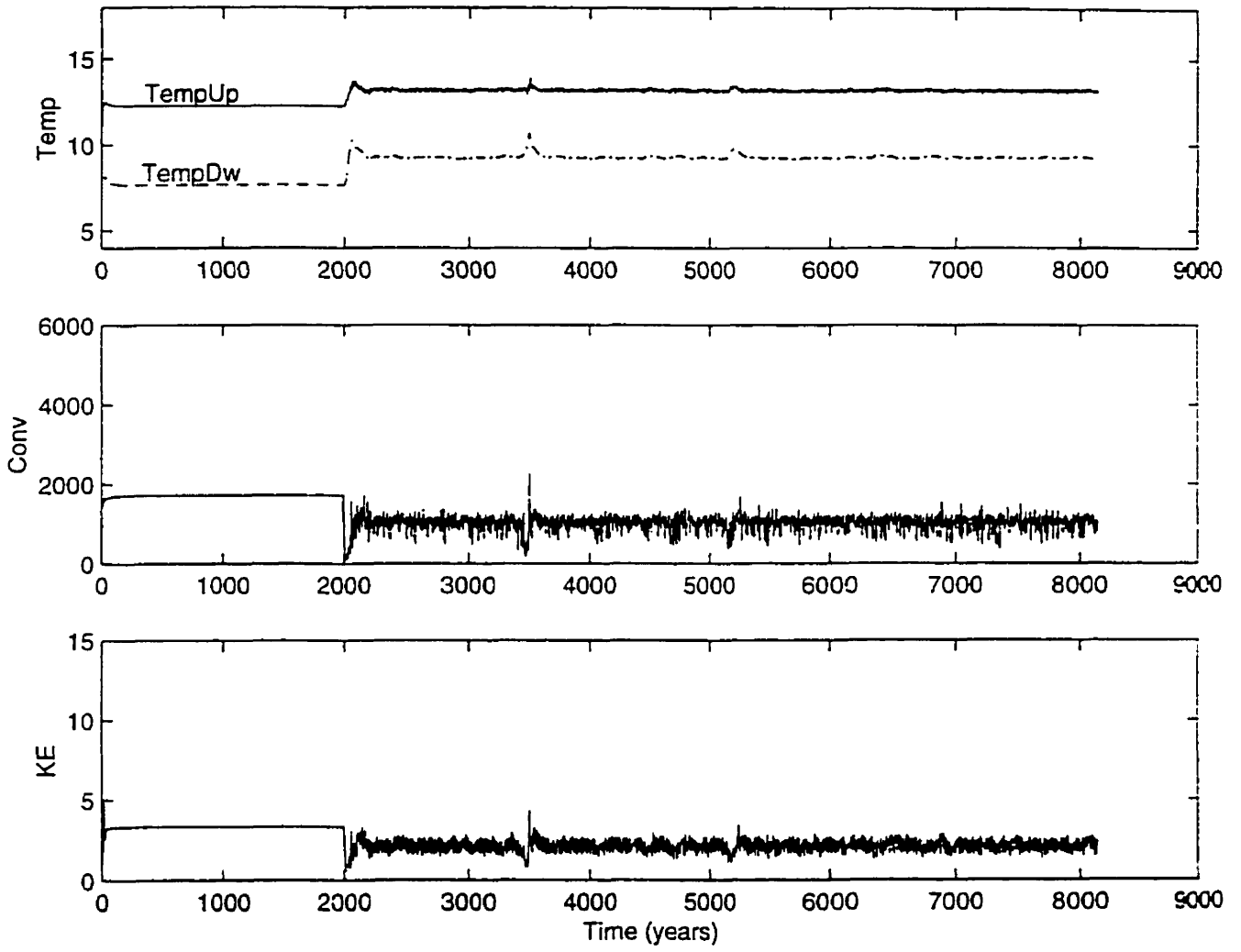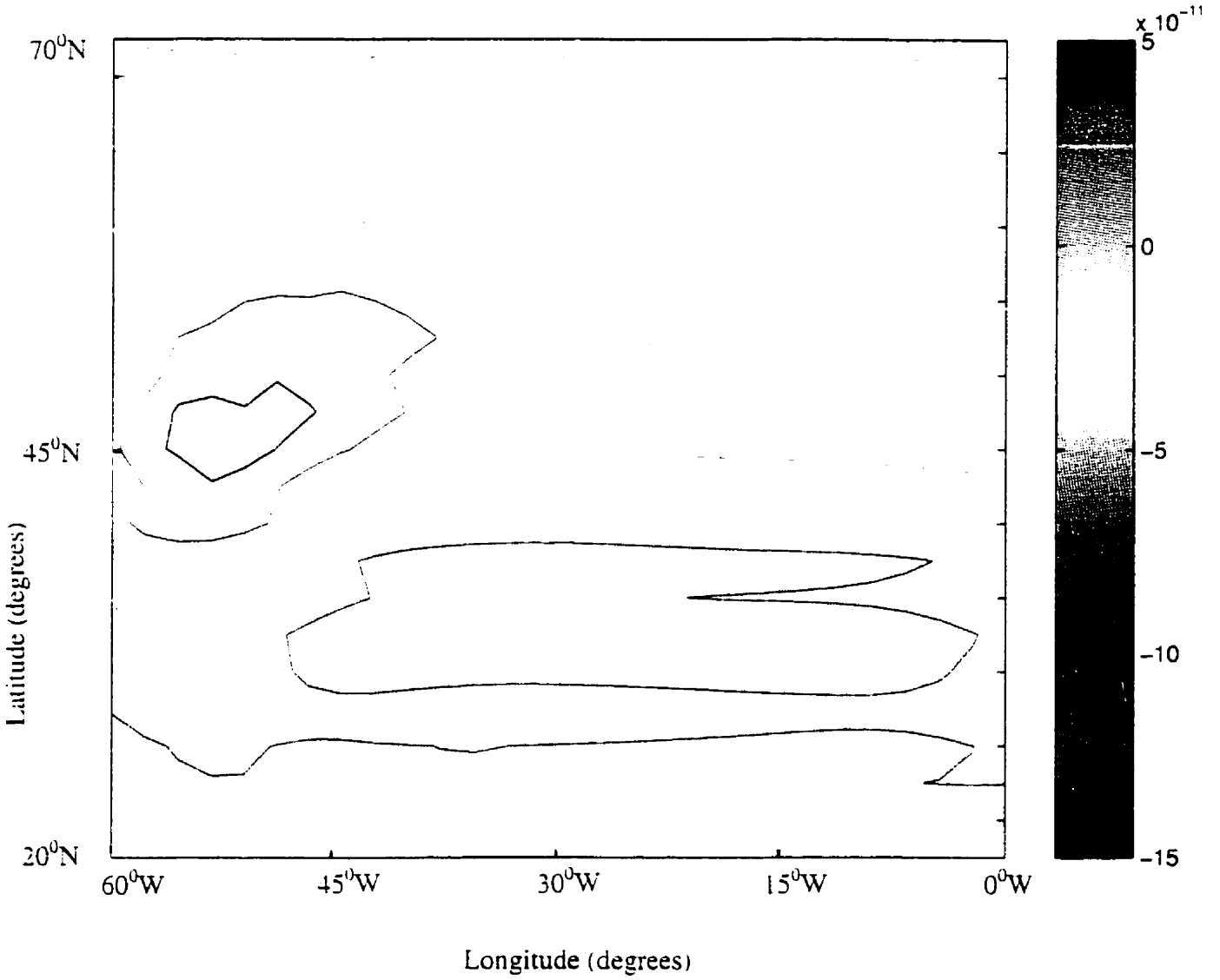
Figure 3.6. Example of surface salinity fluxes (case 19). The salinity flux is in units of parts per second.

Table 3.4. Salt fluxes and model behavior.

Case	Behavior type	Salt fluxes	$A_{DH}(10^7 cm^2/s)$
16	HFO	2.37	0.844
13	HFO	2.24	0.492
10	S	2.16	1.276
20	HFO	2.15	0.688
22	S	1.86	1.668
21	O	1.83	2.452
19	S	1.83	2.060
17	O	1.69	3.040
3	O	1.65	1.080
4	S	1.61	1.864
1	O	1.49	2.648
25	O	1.34	3.432
23	O	1.31	4.020
24	O	1.31	4.216
11	O	1.28	3.326
2	E	1.23	4.608
12	O	1.19	3.824
9	O	1.10	2.256
7	O	1.04	5.000
8	E	0.94	4.412
18	O	0.72	4.804
15	E	0.45	3.628

Figure 3.7. Estimated main effects of salt flux (FS3): (a) vertical eddy diffusivity (A_V); (b) horizontal eddy diffusivity (A_H); (c) vertical eddy viscosity (A_MV); (d) horizontal eddy viscosity (A_MH); and, (c) wind stress (Tau_m).
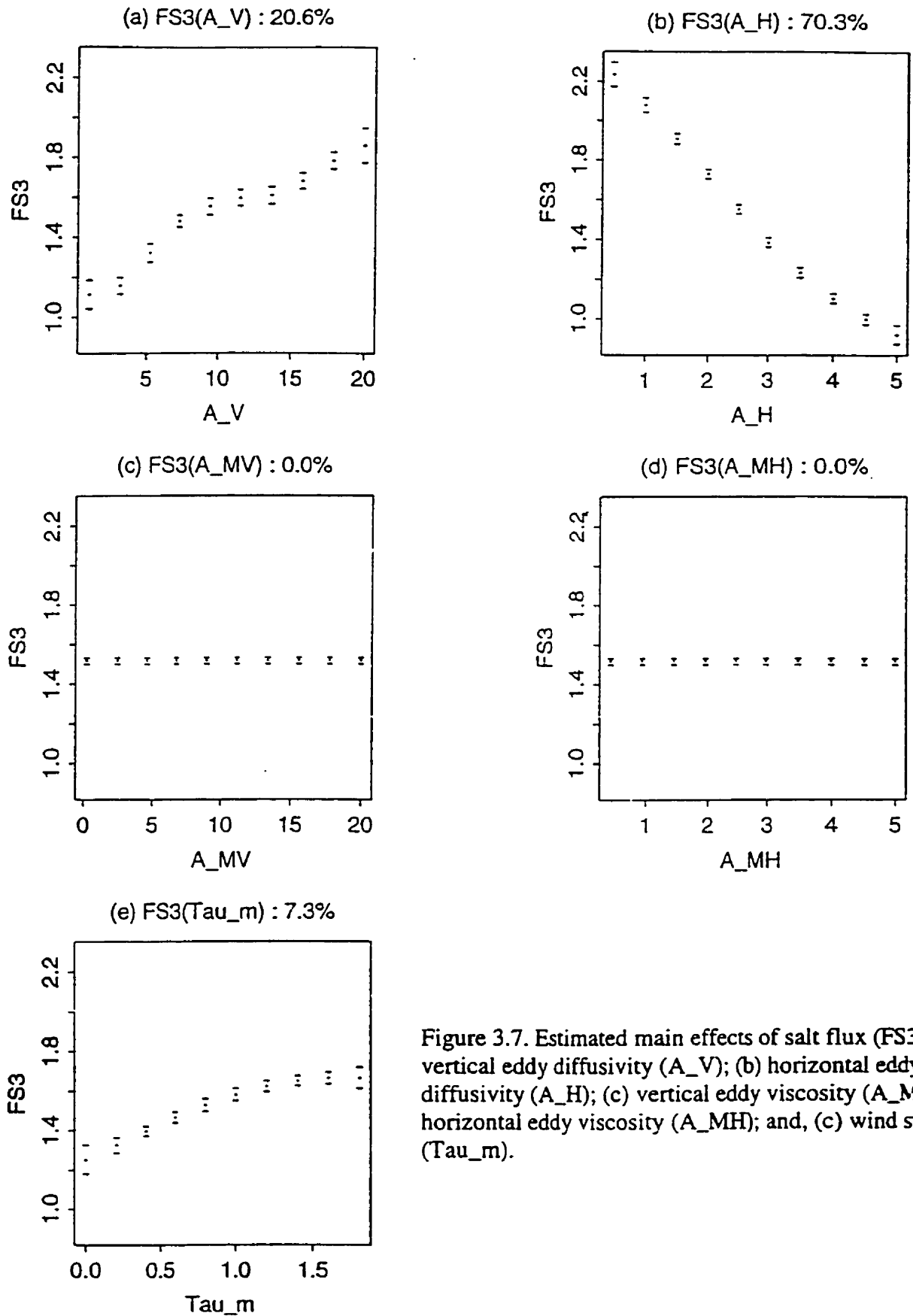
the horizontal diffusivity above which oscillations are damped out. They also show that horizontal diffusion controls the regularity of the oscillation, its amplitude, and period. In all of their models, increasing the horizontal diffusion smooths the horizontal gradients of temperature and reduces the horizontal velocities, hence the mean KE (Bryan 1987). Regarding the variability, increasing the horizontal diffusivity lengthens the oscillation period and reduces its amplitude. The strong influence of horizontal diffusion is in agreement with the advective processes (e.g., Weaver and Sarachik 1991b) where density anomalies travel in the polar regions and modify convection, hence the strength of the thermohaline circulation. When diffusion is too strong, these anomalies are diffused before reaching the convection regions. This is analogous to when too fast a relaxation is applied to the surface temperature, thereby damping out any sea surface temperature deviations. Similarly, Chen and Ghil (1996) show that, in their ocean model coupled to an atmospheric Energy Balance Model, the oscillation amplitude is strongly dependent on the horizontal diffusion coefficient for the atmospheric temperature. This plays a role similar to the horizontal eddy diffusivity in the ocean for the damping of sea surface temperature anomalies.

Weaver et al. (1993) have performed a thorough investigation of possible influences on the stability and variability of the thermohaline circulation in a primitive equation model in a flat-bottom sector domain with mixed boundary conditions. They found that the structure and strength of the surface freshwater flux was the dominant factor controlling stability and variability, with stronger surface freshwater flux leading to increased variability.

Table 3.5 lists the O cases in descending order of oscillation period. Also included are the values for the vertical diffusivity, horizontal diffusivity and wind stress. The period decreases with increasing A_{DV} and A_{DH}, although the vertical diffusivity is the dominant factor. The O behavior occurred for the larger values of the A_{DH} (with the exception of case #3). The impact of the wind stress on the period is not clear (see Edwards et al. 1998; Winton and Sarachik 1993). Winton and Sarachik (1993) showed that increased vertical diffusivity favors thermally direct circulations by diffusing the surface temperature gradients down into the interior, while increased horizontal diffusivity increases poleward salt fluxes.

Huck et al. (1999) reported that horizontal diffusion also controlled the regularity of the oscillation, its amplitude and period. In all of their models, increasing the horizontal diffusion smoothed the horizontal gradients of temperature and reduced the horizontal velocities and thus the mean kinetic energy. The diffusive part of the poleward heat transport

Table 3.5. Period of oscillations

Case	Period (y)	Vertical diffusivity $(A_{DV}; cm^2/s)$	Horizontal diffusivity $(A_{DH}; 10^7 cm^2/s)$	Wind stress $(\tau_m; dynes/cm^2)$
9	2655	3.41	2.256	0.432
25	1281	7.36	3.342	1.224
18	1222	8.15	4.804	0.216
11	1096	10.52	3.236	0.504
1	1047	4.99	2.648	1.584
12	751	12.89	3.824	0.720
24	560	16.05	4.216	1.080
3	546	1.83	1.080	0.864
7	539	16.84	5.000	0.576
17	395	18.42	3.040	0.792
23	383	20.00	4.02	0.360
21	340	15.26	2.452	1.296

also increased while the deep waters warm and the surface waters cooled. This follows since diffusion at high latitudes, where gradients are strong, artificially transports relatively warm waters poleward into the convective regions, thus forming relatively warm bottom water. The reduced surface temperatures are due to the reduced poleward heat advection. Regarding the variability, increasing the horizontal diffusivity lengthened the oscillation period and reduced its amplitude. These results were consistent with the conclusions of Huang and Chou (1994).

3.3.3 Initial conditions

In order to examine the influence of initial conditions in determining model behavior, a new initial condition was introduced for all of the experiments. Instead of the steady state conditions at the end of the spin up phase, the model runs with mixed boundary conditions were integrated with an isothermal and isohaline initial condition. It was found that no qualitative and only minor quantitative differences appeared. These experiments showed that the impact of the initial conditions in determining model behavior is the least important of the factors considered in this study.

3.3.4 Examination of the steady state cases

For the steady state cases (#4, 10, 19, 22), additional experiments were run with the magnification factor of the salinity flux increased from 1.5 to 2.0. These experiments were run to test the hypothesis that increasing the salinity flux would reveal a threshold where the steady state can no longer be maintained and oscillatory behavior sets in. Implementing a flux factor of 2.0 produced oscillatory behavior in all four cases. This confirmed that there is a threshold for oscillatory behavior and that this is a function of the internal parameters.

3.4 Conclusions

In the first set of experiments, a five input parameter space of the ocean model was thoroughly explored using statistical techniques. Statistical analysis enabled the creation of approximating functions to represent the ocean model. These were used to determine the importance of various inputs on the value of a number of model outputs. The outputs were all zero dimensional quantities. The cross validation analysis showed that the statistical approximating function performed well thus allowing reasonable confidence in the analysis of important outputs.

The statistical approximating functions reproduced known model sensitivities. In particular, scaling relationships between the vertical eddy diffusivity and the meridional overturning streamfunction, the northward heat transport and the zonal overturning streamfunction were within values reported in the literature (Bryan 1987; Colin de Verdiere 1988; Bryan 1991; Winton 1996; Gough and Allakhverdova 1998). In addition, the dependence of the overturning streamfunction on the horizontal eddy diffusivity was examined. It was confirmed that the use of the peak value of the streamfunction is not the most representative value to use in determining the strength of the overturning flow.

In the second analysis, it was shown that a wide variety of model behavior occurs when using the same initial restoring boundary conditions (a particular fixed climate). For all of the experiments, the same climatological values were used during the spin up runs and the methodology implemented for mixed boundary conditions was consistent. By simply changing the tunable model parameters (i.e., diffusivities, viscosities and wind stress), four general types of model behavior were produced with enhanced salinity flux surface boundary conditions. The range of observed model behavior included explosive, steady state, high frequency oscillations, and long period oscillations (see Section 3.3.2). The model displayed S behavior for tunable parameter values typically used in modeling studies. In previous work, a variety of model behavior was found mainly by adjusting idealized salinity fluxes (Weaver et al. 1993; Winton and Sarachik 1993; Cai 1995; Chen and Ghil 1995; Yin and Sarachik 1995). In contrast, the salinity fluxes used in this study were the two-dimensional fields produced from the spin up runs. Other studies have tended to use zonally averaged spin up fluxes or idealized fluxes that trivialize the zonal variability of the freshwater fluxes. Repeating the experiments with an isothermal and isohaline initial condition did not produce any qualitative changes. This confirmed the idea that the initial conditions are the least important factor in determining model behavior in this study.

The horizontal diffusivity was found to be the most important model input in determining the nature of the model's response to enhanced salt fluxes. This finding is contrary to Yin and Sarachik (1995) who reported that interdecadal oscillations in the model are mainly a convective and advective phenomenon insensitive to the horizontal diffusivity. They concluded that changes in either surface freshening or subsurface heating will alter the period of the oscillation, while the period of the interdecadal oscillation is not sensitive to the horizontal diffusivity.

The oscillation period was primarily a function of the vertical diffusivity. Similarly, Winton and Sarachik (1993) showed increasing the vertical diffusivity favored thermally direct circulations by diffusing the surface temperature gradients down into the interior. Increasing the vertical diffusivity accomplished a flip by a cooling of the polar ocean through the surface. These authors found that this cooling was at a maximum at the polar boundary. In their model, the resulting meridional density gradients caused a thermally direct cell to strengthen and rise to the surface, eventually importing sufficient salt for deep convection to begin. In addition, a high vertical diffusivity decreased the deep ocean diffusive time scale and reduced the length of the collapsed phase of a deep decoupling oscillation.

The stabilizing effect of wind stress shown in this study is consistent with other work. For example, Yin and Sarachik (1995) found that the regime of model interdecadal oscillations is sensitive to variations in wind stress (Chapter 1, Section 3.1). Winton and Sarachik (1993) also showed that increasing the wind stress stabilized oscillating solutions. In their model, the horizontal transports reinforce the thermally direct circulation by providing heat and salt to the polar region to maintain convection while allowing the overturning to adjust to balance the deep heat budget.

A closer examination of the steady state cases showed that using a flux factor of 2.0 rather than 1.5 produced oscillatory behavior in all four cases. This supported the idea that there is a threshold for oscillatory behavior that is a function of the internal parameters.

4. The influence of varying surface boundary conditions on the oscillatory behavior of an ocean general circulation model

4.1 Introduction

The purpose of these experiments is to examine how simple changes in the surface boundary conditions of an ocean-only model can dramatically influence the resulting thermohaline circulation. To address this research question, the design of the model simulations from the previous section (Chapter 3) was used, but systematic modifications were made to the surface boundary conditions. In Chapter 3, four behavior types were produced by simply changing the tunable model parameters while using the same restoring boundary conditions, based on Levitus (1982), and implementing mixed boundary conditions with two-dimensional surface salinity fluxes. In this section, the Levitus cases were repeated, but with zonally averaged salinity fluxes. In addition, new experiments were conducted where the Levitus restoring boundary condition was replaced with a new sine distribution for restoring temperature and salinity (Figure 4.1a,b). The sine cases included experiments for both two-dimensional surface salinity fluxes and zonally averaged salinity fluxes. The procedure described above permitted the exploration of two main themes: 1) an analysis of how zonally averaging the surface salinity flux impacts the model behavior; and 2) an examination of the impact of a new (sine) distribution of temperature and salinity in determining the nature of the model circulation. An effort was made in this work to gain a greater understanding of the physical mechanisms causing variability of the thermohaline circulation under simple boundary conditions.

4.2 Methodology

From the original set of experiments described in Chapter 3, examples of the four behavior types were selected and spun up to an equilibrium state using Levitus and sine restoring boundary conditions. The prescribed boundary conditions determine the restoring density (Figure 4.1c) through the equation of state (Eq. 2.7) which is a nonlinear function of temperature, salinity and pressure. The region of peak density influences the location of convection sites. A variety of equilibria were produced by the spin up runs. The salinity fluxes at equilibrium were diagnosed and magnified by 1.5 before integrating the models for several thousand years using mixed boundary conditions as was done in Chapter 3. Two types of
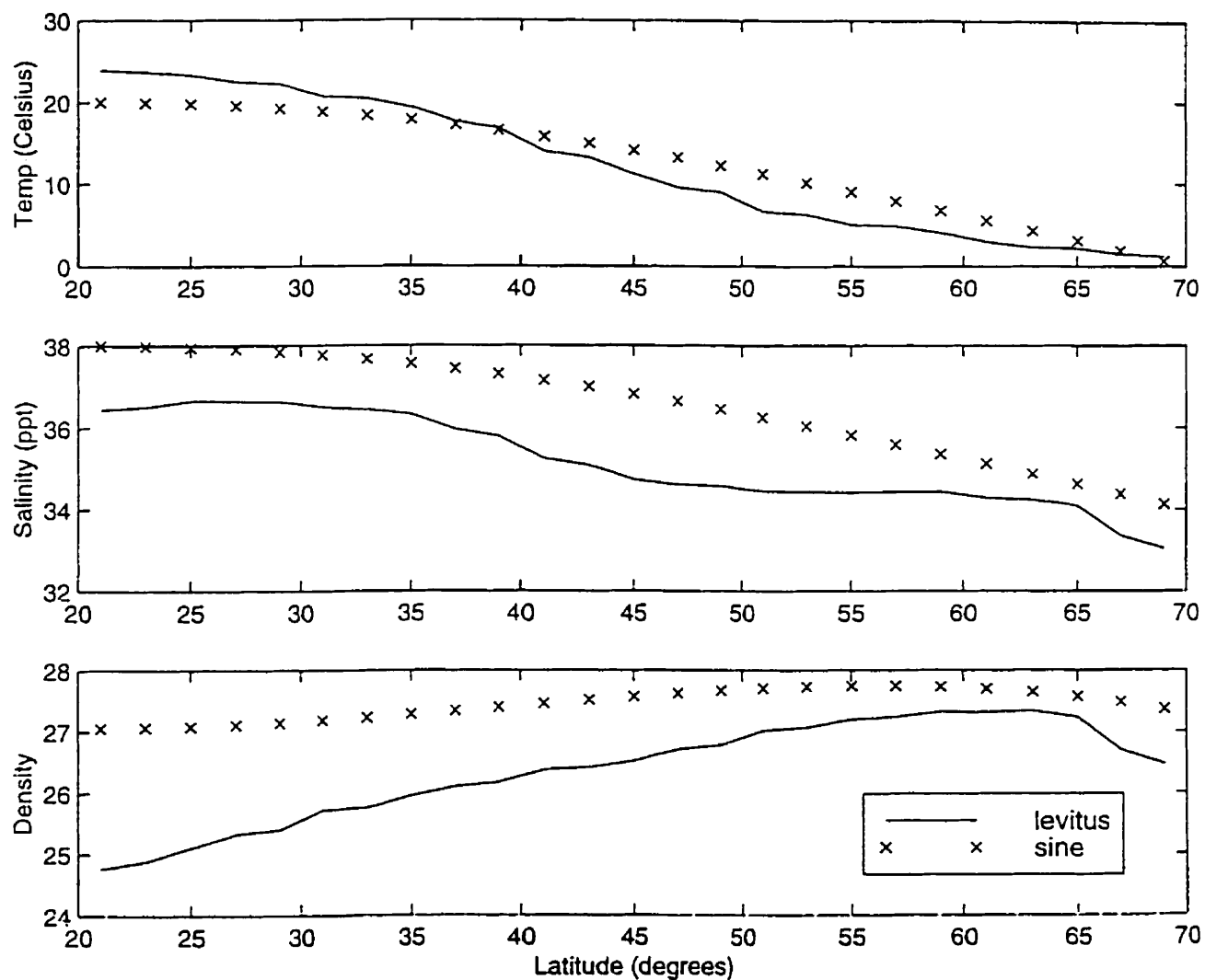
Figure 4.1 Surface restoring values of (a) temperature, (b) salinity, and (c) density. The temperature is in units of Celsius, the salinity in parts per thousand, and the density in sigma representation ($\sigma = \rho - 1000.0$ kg/m^3). (Levitus – solid and sine – x's)

prescribed salinity flux were used in these integrations: 1) a two dimensional salinity flux; and 2) a zonally averaged salinity flux.

4.3 Results and Discussion

4.3.1 Steady state (S) cases

For the steady state cases (#4, 10, 19, 22), the equilibria at the end of the Levitus spin ups typically showed a strong thermally direct circulation with intense downwelling along the northern boundary (Figure 4.2). The peak restoring density for the Levitus runs occurred at approximately 63^0N and this caused intense downwelling in this region. Following the switch to mixed boundary conditions with an enhanced two-dimensional salt flux, the steady state cases exhibited one or two collapses of the thermohaline circulation, but then settled back to a strong thermally direct solution with polar sinking. Case #4 is an exception and it had a considerably smaller value for the strength of the deep overturning (e.g., 10 Sv; 1 Sv = 10^6 m^3/s). This case had a low value for the vertical diffusivity and a high wind stress value.

In comparison to the water mass distribution of the Levitus cases at the end of the spin ups, the steady state cases for the sine runs showed a freshwater cap at the northern boundary (Figure 4.3). Consequently, this cold and fresh polar surface anomaly pushed convection further to the south and the intensity of the thermohaline circulation was reduced. Figure 4.1c shows that the peak restoring density for the sine runs occurred further to the south (at approximately 56^0N) than for the Levitus runs. Overall, the sine cases produced relatively weaker thermally direct solutions during the spin up phase. Under mixed boundary conditions with two-dimensional enhanced salt fluxes, the thermally direct solution was unstable unlike the Levitus cases. The thermohaline circulation underwent oscillations due to the braking effect of a strong salinity forcing and this behavior is similar to the deep decoupling oscillations described by Winton and Sarachik (1993). The polar freshwater cap expanded further to the south and eventually created a polar halocline catastrophe. However, the ensuing thermally direct circulation was sufficiently weak that another freshwater cap developed and this cycle produced oscillatory behavior. The key feature of this behavior, distinguishing it from the Levitus cases, was that the downwelling was weaker and occurred at more southerly latitudes due to the boundary conditions, thus permitting the re-growth of the cold and fresh polar anomaly.

Figure 4.2. Selected model diagnostics zonally averaged at end of spin up run with Levitus restoring boundary conditions (case 22): (a) temperature, (b) salinity, and (c) overturning streamfunction. The temperature is in units of Celsius, the salinity in parts per thousand, and the overturning streamfunction in Sverdrups (1 Sv = 10^6m^3/s).
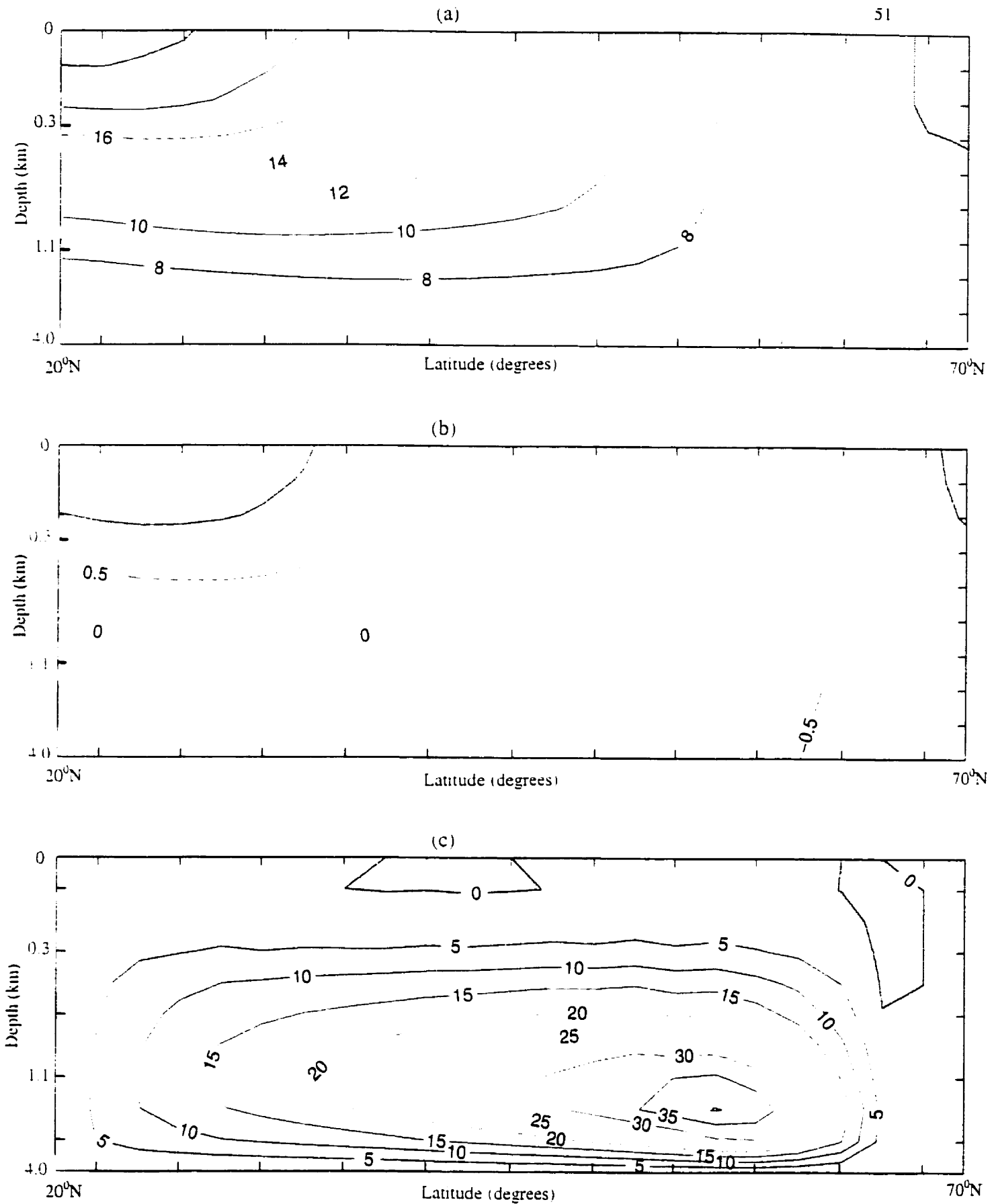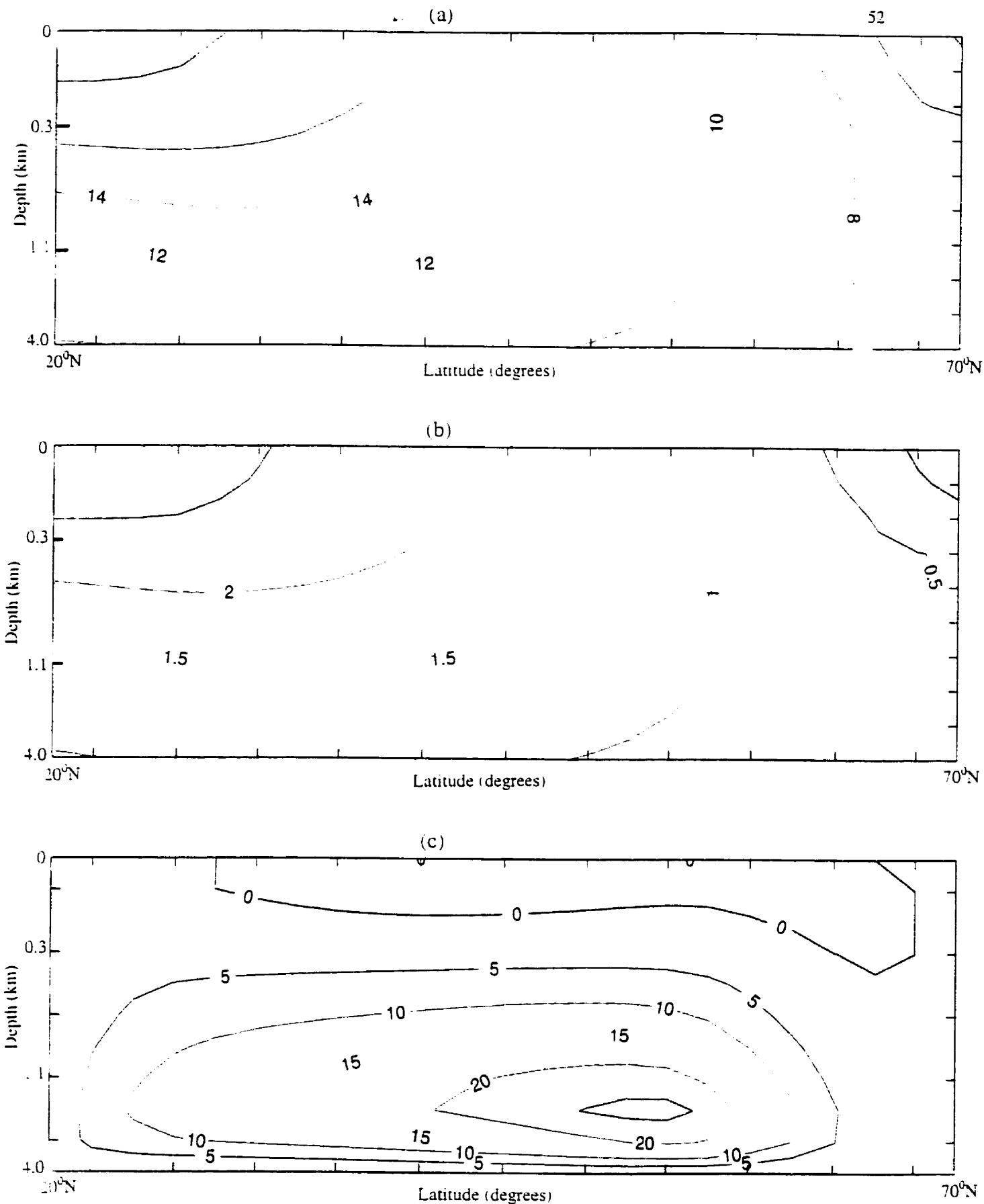
Figure 4.3. Selected model diagnostics zonally averaged at end of spin up run with sine restoring boundary conditions (case 22): (a) temperature, (b) salinity, and (c) overturning streamfunction. The temperature is in units of Celsius, the salinity in parts per thousand, and the overturning streamfunction in Sverdrups ($1\ Sv = 10^6 m^3/s$).

All steady cases were also run with enhanced zonally averaged salinity fluxes. This salinity flux was obtained by taking a zonal average of the two-dimensional salinity flux that was diagnosed and enhanced at the end of the spin up runs. An interesting result for the Levitus steady state cases with zonally averaged salt fluxes was a transition from the steady state equilibrium to a different behavior type (see Table 4.1). The two cases with the lowest wind stress values (#19, 22) switched to HFO superimposed on centennial oscillations. The low wind stress values suggest that the surface wind driven transport of salinity towards the polar region was not strong enough to reinforce a steady circulation with polar sinking. It appears that changing the spatial variability of the model's salinity fluxes induced oscillatory behavior of the thermohaline circulation. As reported by Greatbatch and Zhang (1995) and Huang and Chou (1994), zonally uniform buoyancy fluxes (varying with latitude) can induce decadal oscillations. Cai et al. (1995) noted that a small zonal redistribution of surface buoyancy fluxes, diagnosed at equilibrium under restoring boundary conditions, triggers interdecadal activity. In contrast, Huck et al. (1999), in agreement with and Greatbatch and Peterson (1996), observed that zonal redistribution is not required. Most of the experiments in previous studies were only initialized with the exact equilibrium state after the restoring experiments. As reported in Chapter 3, no qualitative and only minor quantitative differences were found when the Levitus cases employed an isothermal and isohaline ocean as the initial condition for mixed boundary condition runs. Cai et al. (1995), Greatbatch and Peterson (1996) and Huck et al. (1999) noted that oscillations were stimulated by zonally redistributing the diagnosed flux.

The original two-dimensional salinity flux showed a freshwater peak in the midlatitudes by the western boundary. Zonal averaging of the salt flux would increase the freshening in the central and eastern midlatitudes. This would allow fresher water to travel from the central-east region more quickly to the convective area in the northeast corner of the model domain and initiate more convective variability by destabilizing the steady circulation. In contrast, the two-dimensional case had water freshened by the prominent freshwater flux along the western boundary and this freshwater anomaly then traveled northeastward while being diffused and cooled en route to the northeastern corner. This water increased in salinity by diffusive mixing and cooled, hence its density had increased by the time it reached the

Table 4.1 Behavior types and periods of cases for various surface boundary conditions

Run	Levitus, 2D salt fluxes	Levitus, Zonally averaged salt fluxes	Sine, 2D salt fluxes	Sine, Zonally averaged salt fluxes	Comments
10	S	S (minor variablity)	Regular HFO (period=250 y)	Regular HFO (period=100 y)	Zonally averaged salt fluxes produced shorter period oscillations for sine.
22	S	HFO (*decadal and centennial; lots of variability)	Regular HFO (period=100 y)	Regular HFO (period=200 y)	Qualitative change of behavior type.
19	S	O (period=490 y)	HFO (period=200 y)	HFO (period=150 y)	Zonally averaged salt fluxes produced shorter period oscillations.
4	S	S	O (per=2800 y)	O (per > 2500)	Very low A_{DV} (1.04); very high wind stress (1.728).
16	HFO (decadal period)	HFO (decadal; lots of variablity)	HFO (decadal; lots of variability)	HFO (decadal; lots of variability)	Very robust behavior.
13	HFO (decadal and centennial; period=330 y)	Regular HFO (decadal and centennial; period=250 y)	Regular HFO (decadal and centennial; period=300 y)	Very regular HFO (decadal and centennial; period=300 y)	Zonally averaged salt fluxes produced shorter period oscillations for Levitus.
20	HFO (decadal and centennial; period=330 y)	HFO (decadal and centennial; period=300 y)	O (period= 350 y)	O (more variability; period=330 y)	Zonally averaged salt fluxes introduced more variability in O.
21	O (decadal and centennial; period=340 y)	O (period=250)	O (period=200 y)	O (more variability; period=200y)	Zonally averaged salt fluxes produced shorter period oscillations for Levitus.
17	O (very regular; period=400 y)	O (very regular; period=200 y)	O (very regular; period=150 y)	O (very regular; period=150y)	For sine case, not much difference for zonal averaging.
3	O (very regular; period=1150 y)	O (more variability; period=900 y)	O (period=2100 y)	O (period=1900)	Zonally averaged salt fluxes produced shorter period oscillations.
1	O (very regular; period=900 y)	O (very regular; period=350 y)	O (period=1100 y)	O (period=850 y)	Zonally averaged salt fluxes produced shorter period oscillations.
23	O (very regular; period=400 y)	O (very regular; more variability; period=400 y)	O (very regular; period=250 y)	O (very regular; period=200 y; slightly higher KE)	Zonally averaged salt fluxes produced shorter period oscillations for sine.

*decadal and centennial refers to decadal variability superimposed on centennial oscillations

northeastern corner. It appears that zonally redistributing the salinity flux has increased the strength of the salinity flux in our model when considering the location of the important downwelling region in the northeastern corner. Weaver et al. (1993) have performed a thorough investigation of possible influences on the stability and variability of the thermohaline circulation in a primitive equation model in a flat-bottom sector domain with mixed boundary conditions. They found that the structure and strength of the surface freshwater flux was the dominant factor controlling stability and variability, with stronger freshwater flux leading to increased variability.

The two Levitus cases (#4, 10) with the highest windstress values were more robust to changes in the spatial variability of the salinity flux and remained steady with some surficial decadal variability. High windstress reinforces the steady thermally direct solution by transporting salinity poleward at the surface thus maintaining a high surface salinity at the downwelling site where surface water is convected. Edwards et al. (1998) report that wind-induced salinity advection can radically reduce the length of the collapsed phase by destabilizing the northern halocline. Winton and Sarachik (1993) reported that increasing the wind stress and the horizontal diffusivity, while forcing with fixed salinity fluxes, stabilizes oscillating solutions.

As described above, the sine cases were oscillatory and exhibited a cycle of development including a freshwater cap, deep diffusive warming, and a cooling flush. In examining the two-dimensional structure of the salinity flux, it was found that the sine cases do not have the strong midlatitude freshwater flux along the western boundary. The switch to zonally averaged salinity fluxes typically produced only a quantitative change in behavior. It is likely that the zonal redistribution of the salinity flux increased the freshening to the central-east region thus enhancing freshwater transport to the northeastern downwelling site.

It appears that the steady state behavior is very sensitive to the surface boundary conditions and requires a peak restoring density located sufficiently to the north to prevent the development of a stable freshwater cap. This is consistent with the results reported in Chapter 3 where oscillatory behavior was found in all steady cases when the magnification factor of the salt flux was increased from 1.5 to 2.0.

4.3.2 High frequency oscillation (HFO) cases

With two-dimensional salinity fluxes, two of the Levitus HFO cases (#13, 20) exhibited decadal activity superimposed on centennial oscillations. By substituting the zonally averaged salinity fluxes, the period of the centennial oscillations was shortened. The same mechanism described above (Section 4.3.1) applies to these experiments because an increase in the freshwater flux in the central-eastern midlatitudes allowed fresher water to be advected to the northeastern convective region. The increased transport of buoyant water into the downwelling site interrupted convection and shortened the period of the deep decoupling oscillations.

An interesting feature of the sine HFO cases with centennial deep decoupling oscillations (#13,20) was the appearance of less decadal variability than the Levitus cases. In examining the two-dimensional surface salinity fluxes for the Levitus cases (Figure 4.4a) and sine cases (Figure 4.4b) it is clear that the sine cases were more zonally homogeneous. The zonally homogeneous salinity fluxes decreased the FS value and suppressed high frequency oscillations. Zonal averaging of the sine two-dimensional salinity fluxes did not have a significant impact on the qualitative or quantitative behavior of the circulation. Similarly, as described in Chapter 3, a strong freshwater flux along the western boundary promotes surficial oscillations with a decadal time scale in the midlatitudes. The sine two-dimensional salinity fluxes already have low zonal spatial variability and the impact of zonal averaging therefore was only minor.

Case #16 displayed significant quantitative and qualitative changes resulting from alteration of the surface boundary conditions. This case had a high vertical diffusivity and low horizontal diffusivity. This case also had the highest FS value meaning that the salt flux field was highly structured and this was very conducive to localized oscillations. The Levitus case with a two-dimensional salt flux field exhibited random decadal variability at the ocean surface superimposed on a steady thermally direct circulation (Figure 4.5). The zonally averaged case showed that more energetic decadal variability was influencing the deep waters (Figure 4.6). The sine case with a two-dimensional salt flux produced the opposite circulation- a haline dominated circulation with decadal variability. The sine case with zonally averaged salinity fluxes was qualitatively the same, but more energetic. This case demonstrated that introducing a subtle change in the boundary conditions, by substituting a sine distribution in place of the Levitus values, resulted in a dramatic change in the circulation.
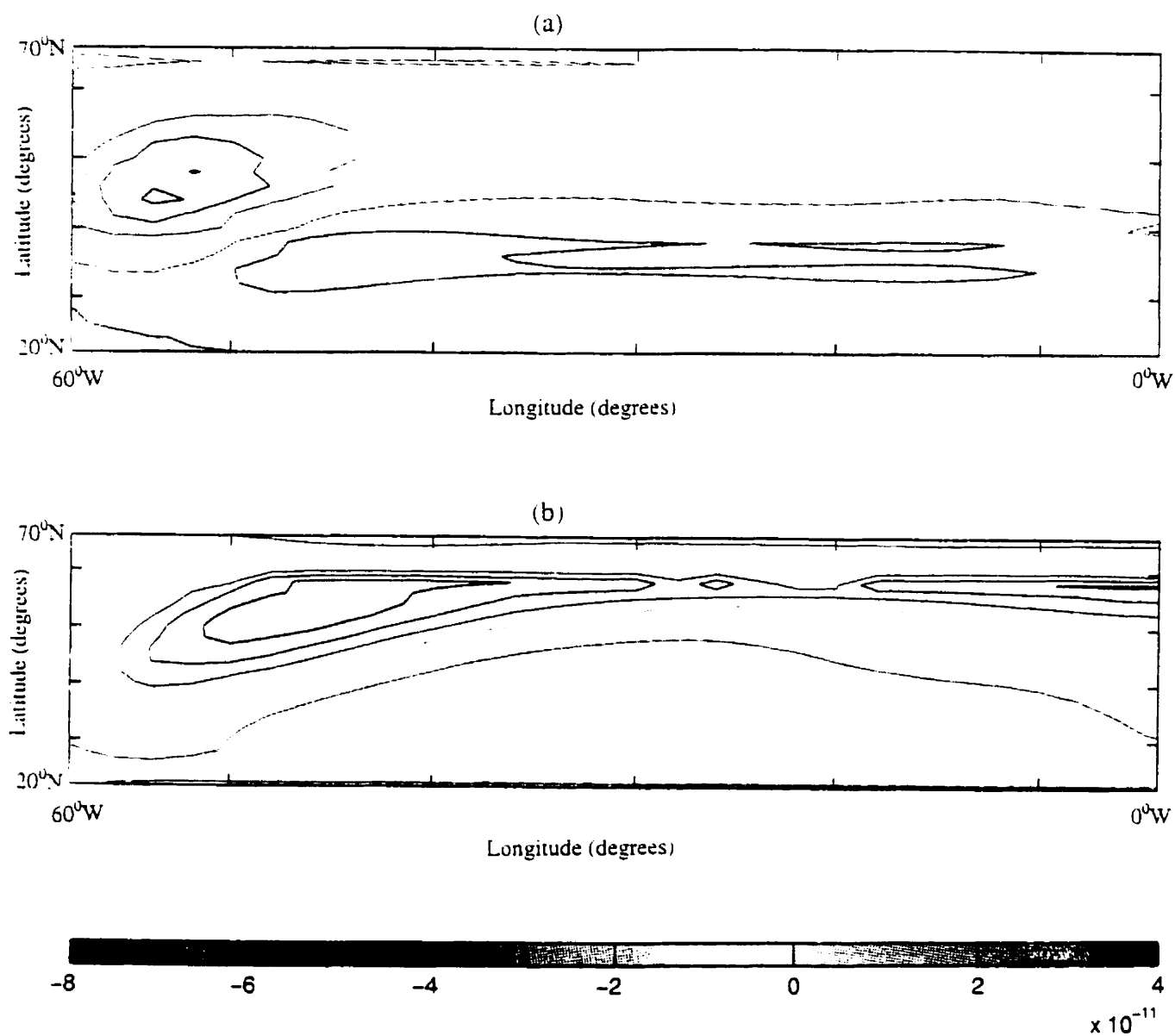
Figure 4.4. Two-dimensional surface salinity fluxes obtained from (a) Levitus restoring boundary conditions and (b) sine restoring boundary conditions. The salinity flux is in units of parts per second.
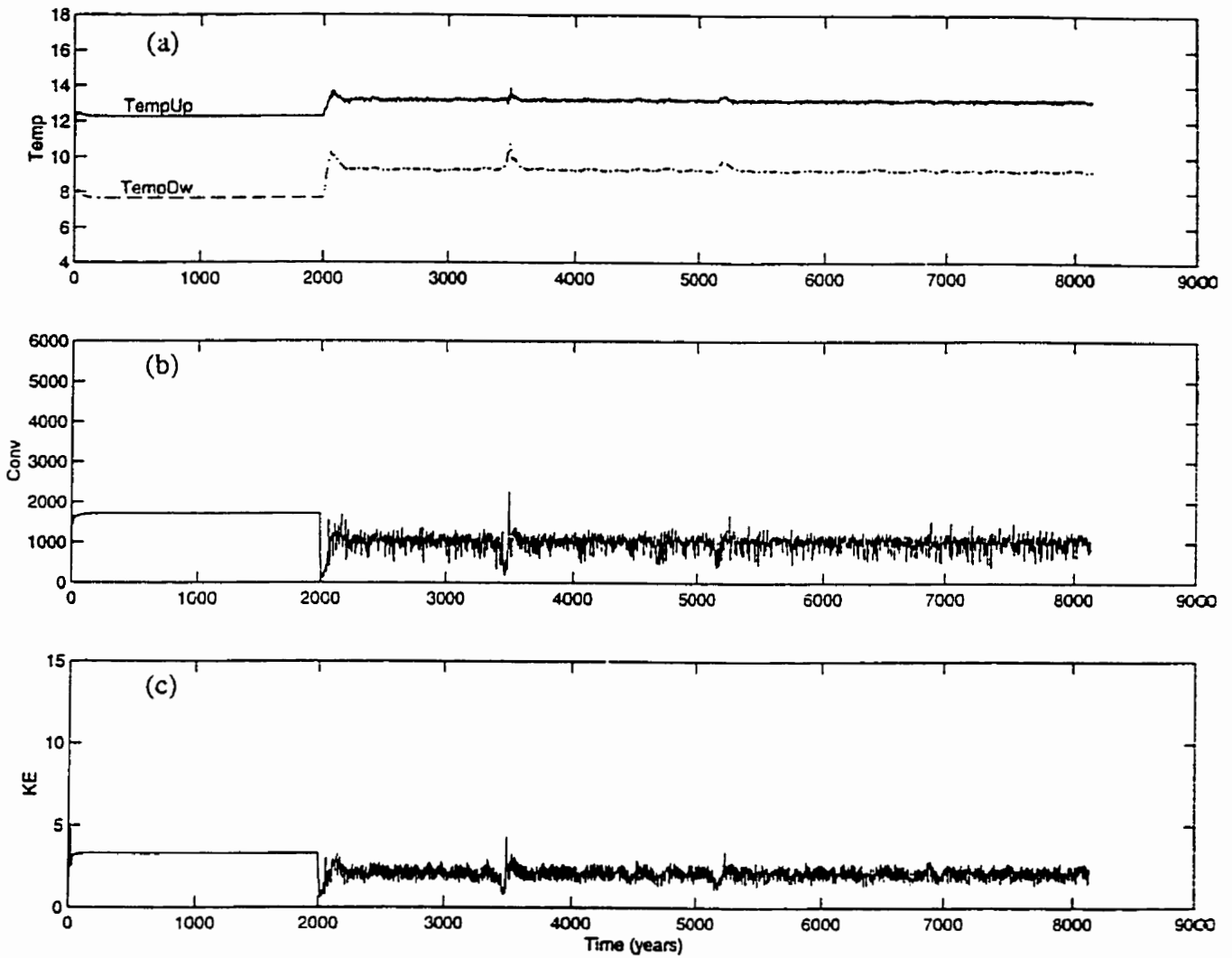
Figure 4.5 Time series of model behavior for case 16 with two-dimensional salt fluxes and Levitus boundary conditions: (a) bottom temperature, (b) number of convection points, and (c) kinetic energy density. The bottom temperature is in units of Celsius, the other measures of model flow are zero dimensional
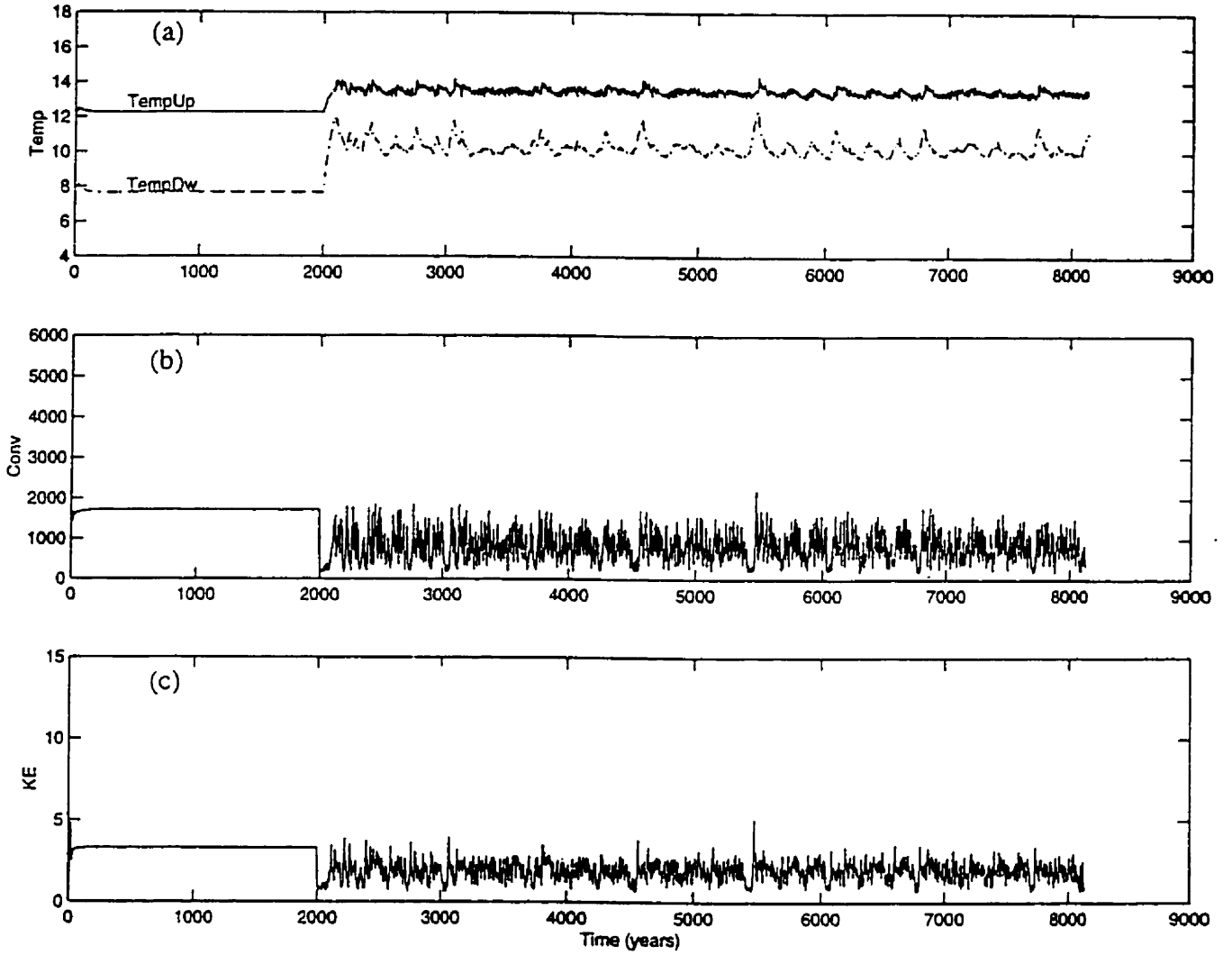
Figure 4.6 Time series of model behavior for case 16 with zonally averaged salt fluxes and Levitus boundary conditions: (a) bottom temperature, (b) number of convection points, and (c) kinetic energy density. The bottom temperature is in units of Celsius, the other measures of model flow are zero dimensional

To illustrate the relative importance of the salt flux and the internal model parameters, case #16 was forced with artificial two-dimensional salt fluxes from all of the remaining cases. A variety of behavior was observed. One case, #15, resulted in a steady state. The other cases displayed a spectrum of decadal, decadal/interdecadal, and less than decadal oscillatory behavior. No centennial or millenial oscillations resulted. This illustrates the dual importance of the salt flux and the values chosen for the internal parameters.

4.3.3 Long period oscillation (O) cases

The effect of zonally averaging the salinity fluxes for the Levitus O cases was to reduce the length of the period. This response is consistent with the mechanism described above (see Section 4.3.1). The increased surface freshwater transport to the northeastern corner destabilizes the overturning and promotes the growth of a freshwater cap thereby inducing a collapse more quickly.

The sine boundary conditions with a two-dimensional salinity flux typically displayed a shortened period. As described above (Section 4.3.1) the sine boundary conditions shift the downwelling site further to the south. This facilitates the development of a freshwater cap along the northern boundary and thus decreases the period of the oscillatory behavior. Zonal averaging the salinity flux consistently reduced the period of the oscillations due to increased freshwater transport from the central-eastern midlatitudes to the convective sites (Section 4.3.1).

4.4 Conclusions

The Levitus cases had diagnosed two-dimensional salinity fluxes that were strongly intensified in the western regions, and a relationship appears to exist between the stability of the circulation and the surface fluxes over this area. Zonally uniform salinity fluxes pushed two steady Levitus cases (#19, 22) into a qualitatively different behavior type characterized by centennial-scale oscillations of the thermohaline circulation. Downwelling was inhibited by the transport of buoyant water from the central-east region into the northeastern corner, and a temporary collapse of polar sinking occurred. With the sine experiments, the same mechanism caused the steady cases with two-dimensional and zonally uniform salinity fluxes (both featured zonally homogeneous salinity fluxes as discussed above) to switch to centennial-scale oscillations. The Levitus cases with two-dimensional salinity fluxes

demonstrated the sensitivity of the steady state circulation to the freshwater flux distribution. The steady state solution was easily destabilized by smoothing the variability of the salt flux field by: 1) imposing zonally uniform salinity fluxes; or, 2) using a sine distribution of the restoring boundary conditions which produced a more zonally homogenous salt flux field. These findings are consistent with Huck et al. (1999) in that the variability is intensified in the two-dimensional salt flux field experiments compared to the variability under zonally uniform fluxes.

A 1.5 magnification of the equilibrium diagnosed salinity fluxes was used in all of the experiments with mixed boundary conditions. Of the four types of behavior that were generated, only four of these cases (#4, 10, 19, 22) displayed robust steady circulations when the stronger salinity flux was imposed. These cases appeared to have a higher threshold before oscillatory behavior occurred. As reported in Chapter 3, oscillatory behavior was induced in these steady cases when the salinity flux was increased two-fold. It was apparent that a switch to zonally averaged salinity fluxes lowered the threshold value and resulted in oscillatory behavior.

The steady state cases were run with new sine restoring temperatures and salinities and also produced decadal-centennial oscillations. This can be attributed to two mechansisms: 1) the sine salinity fluxes were more zonally homogeneous, compared to the Levitus runs, and did not form a strong freshwater flux in the midlatitudes along the western boundary; 2) the sine boundary conditions created a convection region further to the south than the Levitus boundary conditions thus facilitating the development of a fresh polar surface anomaly.

The sine cases showed the importance of the salinity fluxes in generating oscillations rather than the flow field (i.e., due to the internal parameters). It was demonstrated that, for a given set of internal parameters, oscillations could be generated by different surface salinity fluxes. The steady state cases were particularly susceptible to this aspect, compared to the O and HFO cases.

The two Levitus steady cases that were more robust to reduced spatial variability of the salt fluxes were cases #10 and 4. These cases had high values for the wind stress and this destabilized the formation of a freshwater cap by sending greater salinity transport from southern latitudes and preserved the thermally direct solution. It appears that higher wind stress produced a steady state that was more robust to a stronger salt forcing as a result of zonal averaging of the salt flux.

The O cases and HFO cases showed quantitative changes in behavior upon switching to zonally averaged salt fluxes. Switching the Levitus restoring boundary conditions to sine restoring boundary conditions caused the overturning period of the thermohaline circulation to decrease. In general, reducing the zonal variability of the salinity fluxes, either by zonal averaging or by imposing sine boundary conditions, increased the strength of the salt forcing and led to shorter period deep decoupling oscillations.

Finally, the experiments with case #16, when forced with fluxes from all the other cases, illustrated the dual importance of the salt fluxes and the internal parameters. The results included a steady case and showed a spectrum of oscillatory behavior below the centennial time scale.

5. The role of topography on stability of the thermohaline circulation

5.1 Introduction

The purpose of this section is to examine the effect of simple variations in bottom topography on the original simulations described in Chapter 3. The topographic variations were a shoaling toward the pole (north sloping), a shoaling toward the southern boundary (south sloping), a shallowing toward either the eastern or western boundary (east, west sloping), or a shallowing toward all of the north, west and east boundaries (bowl-shaped). The shoaling of the topography was from an ocean depth of four thousand metres to two hundred metres over seven grid points. Test cases of the four behavior types described in Chapter 3 were selected and run with the five new topographic configurations. The standard spin up procedure was implemented followed by diagnosing the salinity flux and applying mixed boundary conditions for the duration of the integration. The restoring temperatures and salinities are based on the Levitus (1982) climatological records and two-dimensional salt fluxes were applied following the spin up. These simulations are intended to improve understanding of the effects of topography and of the behavior of the model in general.

5.2 Results and Discussion

5.2.1 High frequency oscillatory (HFO) cases and long period oscillatory (O) cases

For the O cases in this study, the north and west sloping models typically caused a shortening of the oscillation period (Table 5.1). This destabilizing effect is consistent with Edwards et al. (1998) who suggested that large-scale slope up toward the north or the west can significantly destabilize the circulation by reducing the depth of convection. Two interesting exceptions (cases #1, 3) involved a switch of behavior type to a steady state circulation when the north sloping topography was introduced. A comparison of the diagnosed salinity fluxes for these two cases with the other long period oscillation cases showed that the peak freshwater flux occurred slightly further to the south and there was net salting along the northern boundary. Coupled with the north sloping model, this configuration of the salt flux field appears to have produced a more robust overturning circulation. Figure 5.1 shows the diagnosed surface salinity fluxes of a case that switched to a steady state circulation (case #1) and a case that maintained long period oscillations (case #21). In contrast to the O cases, north and west slopes had a stabilizing effect on the HFO cases. Several of

Table 5.1. Behavior types and periods of cases for various topographies.

| Run	Flat bottom	North sloping	West sloping	South sloping	East sloping	Bowl-shaped
10	S	O (regular; period=300 y)	S	O (regular; period=300 y)	O (decadal and centennial variability; period=150 y)	O (regular; period=150 y)
22	S	O (decadal and centennial variability; period=300 y)	O (decadal and centennial variability; period=350 y)	HFO (decadal)	HFO (decadal)	O (period=200 y)
19	S	S	S	O (very regular; period=450 y)	O (very regular; period=200 y)	O (period=170 y)
4	S	S (surficial decadal variability)	O	O (period=1700 y)	O (per>1000 y)	S
16	HFO (decadal)	S (decadal variability during spin up)	S (surficial decadal variability)	HFO (decadal-centennial)	HFO (decadal-centennial)	O (decadal and centennial variability; period=150 y)
13	HFO (decadal and centennial variability; period=330 y)	S (surficial decadal variability)	O (period~1000 y)	HFO (decadal and centennial variability; period=300 y)	HFO (decadal and centennial variability; period=200 y)	HFO (decadal and centennial variability; period=250 y)
20	HFO (decadal and centennial variability; period=330 y)	O (lots of variability; period=900 y)	S (some surficial variability)	HFO (decadal and centennial variability; period=200 y)	HFO (decadal and centennial variability; period=200 y)	HFO (decadal and centennial variability; irregular period; period~300 y)
21	O (some decadal variability; period=340y)	O (regular; period=300 y)	O (regular; period=250 y)	O (regular; period=350 y)	O (regular; period=250 y)	O (regular; period=150 y)
17	O (very regular; period=400 y)	O (regular; period=250 y)	O (regular; period=250 y)	O (regular; period=450 y)	O (regular; period=220 y)	O (regular; period=150 y)
3	O (very regular; period=1150 y)	S	O (period=650 y)	O (period=600 y)	O (period=400 y)	O (period=460 y)
1	O (very regular; period=900 y)	S	O (period=400 y)	O (very regular; period=350 y)	O (very regular; period=250 y)	O (very regular; period=300 y)
23	O (very regular; period=400)	O (decadal and centennial variability; period=200 y)	O (very regular; period=300 y)	O (very regular; period=310 y)	O (very regular; period=210 y)	O (very regular; period=170 y)
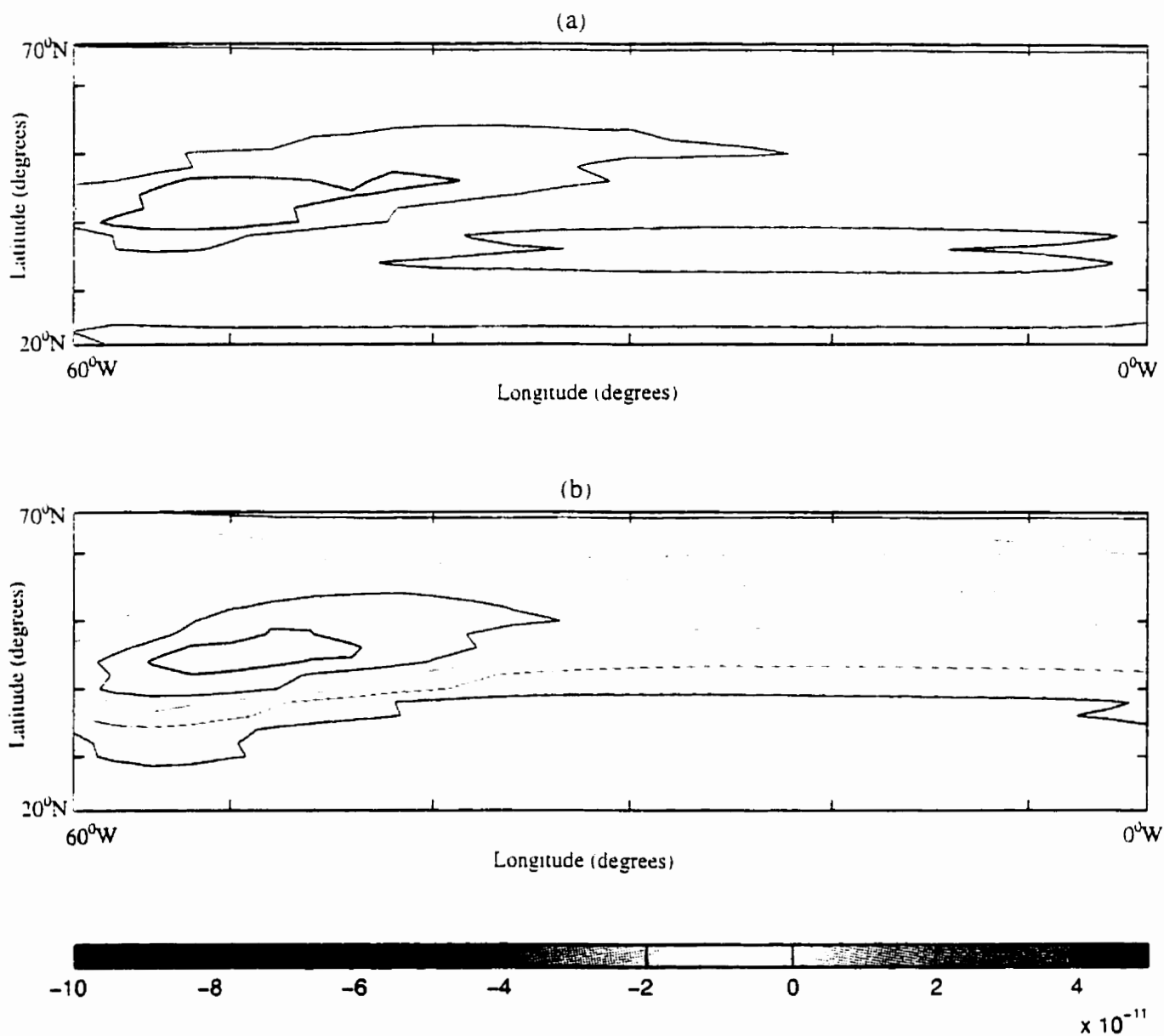
Figure 5.1. Diagnosed surface salinity fluxes for two long period oscillatory cases: (a) case 1, and (b) case 21. The salinity flux is in units of parts per second.

these cases exhibited qualitative changes of behavior (switching to steady overturning circulations) and also quantitative changes (centennial oscillation in some cases were lengthened).

The HFO and O cases, for south sloping, east sloping, and bowl-shaped configurations, did not display qualitative changes in behavior. The south sloping variation had the least impact of any alteration on model solutions. The east sloping model and bowl-shaped experiments consistently demonstrated a reduction in period of the deep decoupling oscillations. This is unsurprising for two reasons: 1) the convection region lies in the northeastern corner of the model domain and a reduction in convective depth would shorten the collapsed phase; 2) a reduction in the ocean volume would decrease the time required for diffusive heating of the deep water, instability and a flushing event. As mentioned in Edwards et al. (1998), the overall period of the oscillations is usually governed by the time taken for diffusive warming to destabilize the deep ocean. Winton (1997) showed that decadal oscillations are greatly damped when bowl-shaped bottom topography is included (see also Moore and Reason 1993). The present bowl experiments do not support this claim, but there are important differences between the two methodologies. For example, Winton (1996) reduced the robustness of his results by using fixed heat fluxes and idealized salinity fluxes. A damping influence similar to Winton's (1996) is only apparent in our north and west sloping cases.

In contrast to the findings of Edwards et al. (1998), the west sloping cases are relatively stable for O and HFO cases whereas the east slope introduces significant instability. This observation is opposite to that of Edwards et al. (1998) and, in general, the present results show much more variability. An important point to consider is that Edwards et al. (1998) used highly idealized salinity fluxes in all their experiments. Unlike the zonally averaged salinity fluxes of Edwards et al. (1998), the present study diagnosed two-dimensional salinity fluxes for each case following the two thousand year spin up phase. As shown in Figure 5.1, there is considerable zonal variability in the salt flux field and a particularly prominent freshwater flux in the midlatitudes along the western boundary. It is likely that this more realistic salt flux forcing produces a broader range of behavior better representing the variety of model behavior generated by the system.

5.2.2 Steady state (S) cases

Steady state cases with south, east and bowl-shaped slopes usually changed to long period oscillatory behavior. Case #22 had the lowest wind stress and the highest vertical diffusivity and appeared to be particularly sensitive to a switch to oscillatory behavior due to changes in topography or surface restoring boundary conditions (Chapter 4). Some of the steady equilibria were more robust to north and west slopes and preserved the steady solution under these conditions. Case #4 had a very high wind stress and low vertical diffusivity and was particularly robust to changes in topography or surface boundary conditions (Chapter 4). It appears that wind forcing can promote deep overturning by salinity advection toward the northern wall, thereby inhibiting the development of a fresh polar anomaly and ensuing collapsed phase.

The steady cases with a bowl-shaped topography exhibited deep decoupling oscillations with a centennial time scale. This can be attributed to the mechanism described above (Section 5.3.1) associated with a reduced convective depth and reduced ocean volume. It appears that the steady state behavior type is sensitive to topographic changes. It has been shown in Chapter 3 that the steady circulation exists close to a stability threshold and that slight changes to the salt forcing can destabilize the overturning. The topographic variations in the present study tended to cause qualitative changes of the steady state circulation resulting in both long period oscillations and high frequency oscillations. Some interesting exceptions were two cases (#4, 19) which had more robust steady state circulations and exhibited very limited decadal variability. These cases had relatively large values for wind stress and this would increase advection of salty water to the polar region reinforcing the thermally direct circulation and inhibiting a collapse due to the formation of a polar cap. In addition, these cases had the lowest salt flux values for the steady state cases and this suggests that decadal variability does not tend to occur without a highly structured salt flux field (see Chapter 3).

5.3 Conclusions

The north sloping model is designed to qualitatively represent the northward decrease in average depth of the North Atlantic. The runs with bottom slope to the south, east or west are intended to model generic processes rather than specific oceanographic locations. By implementing more realistic salinity fluxes, the range of model behavior produced in this

investigation is much broader than that reported in other studies (Yin and Sarachik 1995; Winton 1997; Edwards et al. 1998). The two-dimensional salinity fluxes showed considerable zonal variability with a prominent freshwater flux in the midlatitudes along the western boundary.

The bowl-shaped simulations for the long period oscillation cases showed a quantitative change with reduced oscillation periods. In fact, for almost all of the behavior types, the bowl-shaped experiments produced centennial scale deep decoupling oscillations with decadal variability. The HFO cases had considerably more decadal variability and this is associated with the high salt forcing strength in these cases (Chapter 3). In general, the bowl-shaped models cause a reduced volume of the ocean basin and a barrier to convection due to the new topography. Both of these factors contribute to reducing the period of the deep decoupling oscillations. Also, the reduced ocean volume allows the time scale of diffusive heating of the deep water to be shorter.

For the O and HFO cases, the east sloping model consistently shows a significant reduction of the oscillation period. This destabilizing effect is likely related to the importance of the northeastern corner of the model domain as the main downwelling site. The reduction of the convective depth in the east sloping model results in a shorter collapsed phase.

Several cases supported the idea that wind driving can stabilize the steady overturning by salinity advection to the northern wall thereby inhibiting the development of a northern halocline.

6. Conclusions

In this thesis, four main sources of oscillatory behavior in ocean models have been examined: internal model parameters (diffusivities, viscosities), external forcing (wind stress, thermal forcing, freshwater forcing), topography, and initial conditions. Using a primitive equation ocean general circulation model, systematic modifications of these factors were applied and the response of the thermohaline circulation was analyzed. This investigation was designed to highlight how slight changes to basic factors necessary for the configuration of an ocean-only model have a critical impact on the resulting model behavior. The main goal was to examine the response of the model behavior to a range of conditions and to compare these findings to previously published reports. At present, numerical ocean models are widely used in process studies of the ocean and climate change simulations. The validity of these studies is dependent on an understanding of the model being employed, its inherent limitations and the sensitivities that influence the applicability of model output to real world phenomena.

Chapter 3 revealed the point that variation of the internal parameters alone produced a full spectrum of oscillatory behavior. The range of observed behavior included explosive, steady state, high frequency oscillations, and long period oscillations. The same climatological values were used during the spin up for all of these experiments, and only the values of the tunable model parameters (i.e., diffusivities, viscosities and wind stress) differed between the runs. Upon switching to mixed boundary conditions, two-dimensional salinity fluxes were used. Previous studies have typically used zonally averaged or idealized salinity fluxes that tended to trivialize the variability in the diagnosed salt flux field. The results from this study showed that a wider variety of behavior was produced with two-dimensional salinity fluxes compared to the use of artificial salinity fluxes.

In another set of experiments, the spin up runs from Chapter 3, were followed by mixed boundary conditions implemented as described above. However, these extension runs were commenced with an isothermal and isohaline condition. The model behavior showed no qualitative and only minor quantitative changes. This confirmed the idea that the initial conditions have only a minor role in determining the model circulation.

In Chapter 4, it was noted that two-dimensional salinity fluxes produced a broader range of behavior than reported in the literature, supporting the findings reported in Chapter 3. Zonal variability of the salinity fluxes had an important influence on the types of model behavior produced. In particular, a consistent pattern in the two-dimensional salinity fluxes was a peak freshwater flux along the western boundary in the mid-latitudes. The sine experiments also showed the importance of the salt flux distribution in determining model behavior. The salinity fluxes resulting from the sine cases had a different structure than the Levitus cases and this inhibited the development of a strong thermally direct circulation. In fact, all of the steady cases switched to oscillatory behavior when run with sine boundary conditions. Clearly, the more realistic salinity fluxes used in the present investigations on the Levitus data set showed that variability in the model response is damped when idealized salinity fluxes replace the diagnosed salinity fluxes.

An example of the importance of internal parameters in allowing for oscillatory behavior to occur was also demonstrated. In the original run, case #16 exhibited high frequency oscillations and, in subsequent experiments, it was artificially forced by the salinity fluxes diagnosed from all of the other cases. One case resulted in a steady state and the other cases displayed a spectrum of decadal, decadal/interdecadal, and less than decadal oscillatory behavior. These experiments did not produce any centennial or millennial oscillations. This illustrated the dual importance of the salinity flux and the values chosen for the internal parameters in determining model behavior.

An examination of the impact of topography on model behavior also contributed to an understanding of the importance of two-dimensional salinity fluxes. In contrast to other reports where the idealized topography of the model was varied, a broader range of behavior was produced in the present experiments which implemented two-dimensional salinity fluxes. Typically, previously reported studies have used idealized salinity fluxes.

Directions for future research stem from this investigation. For example, the type of experiments described above for case #16 have not been previously reported in the literature and they provide a new avenue to explore the importance of internal parameters. The robustness of the HFO behavior type for case #16, despite the application of a variety of artificial freshwater fluxes, clearly indicated that the internal

parameters play a role in allowing for oscillatory behavior. Whereas most previous studies that have examined oscillatory behavior have focused on the freshwater flux, it is of interest to design experiments that reveal the dual importance of the salinity flux and the values chosen for the internal parameters. Carrying out the same methodology described for case #16 with the remainder of the cases would expand our understanding of this dual effect. An in-depth analysis of the physical mechanisms underlying this behavior would also be of interest.

Another key extension would be to implement double flux boundary conditions (fixed flux for both temperature and salinity) with the experiments described in this study. It has been suggested that mixed boundary conditions lead to artificial behaviors (Zhang et al. 1993) and do not represent properly the large-scale atmosphere-ocean interactions. Several authors, as noted in Chapter 1, have used fixed flux boundary conditions as a simplification of the original mixed boundary condition experiments and have generated purely-oceanic decadal scale variability in their models. A direct comparison of the present results with these previous studies would be possible by repeating the experiments with fixed flux boundary conditions.

A restoring boundary condition on temperature implies a model of an atmophere whose temperature always remains fixed. Coupling the ocean model to a more realistic atmospheric model would allow an examination of the robustness of the results under more sophisticated conditions. Rahmstorf and Willebrand (1995) report that their new thermal boundary condition, derived from an atmospheric energy balance model, had a stabilizing effect on the conveyor belt circulation due to temperature feedbacks (see Section 1.2.2). Although these authors did not investigate the effect of their new thermal boundary condition on internal oscillations of the thermohaline circulation, it is expected that the temperature feedback would also dampen these oscillations. This boundary condition cannot replace a fully coupled ocean-atmosphere model, but it approximated the heat balance of the atmosphere at low computational cost and allows qualitative study of climatic processes with ocean circulation models.

Lastly, a logical next step in this research effort would be to use a coupled atmosphere-ocean model for an analysis of the impact of varying internal parameters on model behavior. In Chapter 3, it was shown that the internal parameters are very

important in determining the resulting model circulation for an ocean-only model. Under coupled conditions, the atmospheric component generates freshwater fluxes and heat fluxes. A comparison of the Chapter 3 results with data generated from a more realistic coupled model would be of interest.

References

Arakawa, A. 1966. Computational design for long term numerical integration of the equations of fluid motion. *J. Comput. Phys.*, 1: 119-143.

Bond, G., W. S. Broecker, S. Johnsen, J. McManus, L. Labeyrie, J. Jouzel, and G. Bonani. 1993. Correlations between climate records from North Atlantic sediments and Greenland ice. *Nature*, 365: 143-147.

Boyle, E. A. and L. Keigwin. 1987. The North Atlantic thermohaline circulation during the past 20 000 years linked to high latitude surface temperature. *Nature*, 330: 35-40.

Bretherton, F. P. 1982. Ocean Climate Modeling. *Progress in Oceanography*, 11: 93-129.

Broecker, W. S. 1987. The biggest chill. *Natural History Magazine*, 96: 74-82.

Broecker, W. S. 1991. The great ocean conveyor. *Oceanography*, 4: 79-89.

Broecker, W. S., D. M. Peteet, and D. Rind. 1985. Does the ocean-atmosphere system have more than one stable mode of operation? *Nature*, 315: 21-26.

Broecker, W. S., G. Bond, M. Klas, E. Clark, and J. McManus. 1992. Origin of the northern Atlantic's Heinrich events. *Climate Dyn.*, 6: 265-273.

Broecker, W. S. and G. H. Denton. 1990. What drives glacial cycles? *Sci. Amer.*, 262: 49-56.

Bryan, F. 1986a. Maintenance and variability of the thermohaline circulation. Ph.D. thesis, Atmospheric and Ocean Sciences Program, Princeton University, 254 pp.

Bryan, F. 1986b. High-latitude salinity effects and interhemispheric thermohaline circulations. *Nature*, 323: 301-304.

Bryan, F. 1987. Parameter sensitivity of primitive equation ocean general circulation models. *J. Phys. Oceanogr.*, 17: 970-985.

Bryan, K. 1969. A numerical method for the study of the circulation of the world ocean. *J. Comput. Phys.*, 4: 347-376.

Bryan, K. 1984. Accelerating convergence to equilibrium of ocean-climate models. *J. Phys. Oceanogr.*, 14: 666-673.

Bryan, K. 1991. Poleward heat transport in the ocean. *Tellus*, 43AB: 104-115.

Bryan, K. and M. D. Cox. 1972. An approximation equation of state for numerical models of ocean circulation. *J. Phys. Oceanogr.*, 2: 510-514.

Bryan, K., S. Manabe, and R. C. Pacanowski. 1975. A global ocean-atmosphere climate model. II. The ocean circulation. *J. Phys. Oceanogr.*, 2: 510-514.

Cai, W. 1995. Interdecadal variability driven by mismatch between surface flux forcing and oceanic freshwater/heat transport. *J. Phys. Oceanogr.*, 25: 2643-2666.

Cai, W. and S. J. Godfrey. 1995. Surface heat flux parameterizations and the variability of the thermohaline circulation. *J. Geophys. Res.*, 100: 10,679-10,692.

Cai, W., R. J. Greatbatch, and S. Zhang. 1995. Interdecadal variability in an ocean model driven by a small, zonal redistribution of the surface buoyancy flux, *J. Phys. Oceanogr.*, 25(9), 1998-2010.

Capotondi, A. and R. Saravanan, 1996. Sensitivity of the thermohaline circulation to surface buoyancy forcing in a two-dimensional ocean model. *J. Phys. Oceanogr.*, 26: 1039-1058.

Chen, F. 1993. Interdecadal-to-centennial variability of an idealized North Atlantic Ocean model. M.S. thesis. University of California, Los Angelas, 89 pp.

Chen, F. and M. Ghil. 1995. Interdecadal variability of the thermohaline circulation and high-latitude surface fluxes. *J. Phys. Oceanogr.*, 25: 2547-2568.

Chen, F. and M. Ghil. 1996. Interdecadal variability in a hybrid coupled ocean-atmosphere model. *J. Phys. Oceanogr.*, 26: 1561-1578.

Colin de Verdiere, A. 1988. Buoyancy driven planetary flows. *J. Mar. Res.*, 46: 215-265.

Cox, M. 1984. A primitive equation, three dimensional model of the ocean. *GFDL Ocean Tech. Report No. 1.* Princeton, New Jersey.

Dansgaard, W., S. J. Johnsen, H. B. Clausen, N. S. Dahl-Jensen, N. S. Gundestrup, C. U. Hammer, C. S. Hvidberg, J. P. Steffensen, A. E. Sveinbjornsdottir, J. Jouzel, and G. Bond. 1993. Evidence for general instability of past climate from 250-kyr ice-core record. *Nature*, 364: 218-220.

Delworth, T., S. Manabe, and R. J. Stouffer. 1993. Interdecadal variations of the thermohaline circulation in a coupled ocean-atmosphere model, *J. Climate*, 6: 1993-2011.

Deser, C. and M. L. Blackmon. 1993. Surface climate variations over the North Atlantic Ocean during winter: 1900-1989. *J. Climate*, 6: 1743-1753.

Edwards, N. R., A. J. Willmott, and P. D. Killworth. 1998. On the role of topography and wind stress on the stability of the thermohaline circulation. *J. Phys. Oceanogr.*, 28: 756-778.

Gordon, A. L. 1986. Interocean exchange of thermocline water. *J. Geophys. Res.*, 91: 5037-5046.

Gough, W. A. 1991. Lateral and isopycnal mixing of passive and active tracers in an ocean general circulation model. Ph.D. thesis. McGill University, Montreal, Canada, 147 pp.

Gough, W. and C. Lin. 1992. The response of an ocean general circulation model to long time-scale surface temperature anomalies. *Atmos.-Ocean*, 30: 653-674.

Gough, W. and W. Welch. 1994. Parameter space exploration of an ocean general circulation model using an isopycnal mixing parameterization. *J. Mar. Res.*, 52: 773-796.

Gough, W. and T. Allakhverdova. 1998. Sensitivity of a coarse resolution ocean general circulation model under climate change forcing. *Tellus*, 50A: 124-133.

Greatbatch, R. J. and S. Zhang. 1995. An interdecadal oscillation in an idealized ocean basin forced by constant heat flux. *J. Climate*, 8: 81-91.

Greatbatch, R. J. and K. A. Peterson. 1996. Interdecadal variability and oceanic thermohaline adjustment. *J. Geophys. Res.*, 101 (C9): 20,467-20,482.

GRIP Members. 1993. Climate instability during the last interglacial period recorded in the GRIP ice core. *Nature*, 364: 203-207.

Grousset, F. E., L. D. Labeyrie, J. A. Sinko, M. Cremer, G. Bond, J. Duprat, E. Cortijo, and S. Huon. 1993. Patterns of ice-rafted detritus in the glacial north Atlantic. *Paleooceanogr.*, 8: 175-192.

Hansen, D. V. and H. F. Bezdek. 1996. On the nature of decadal anomalies in North Atlantic sea surface temperature, *J. Geophys. Res.*, 101: 8749-8758.

Haney, R. L. 1971. Surface thermal boundary condition for ocean circulation models. *J. Phys. Oceanogr.*, 1: 241-248.

Hasselmann, K. 1991. Ocean circulation and climate change. *Tellus*, 43: 82-103.

Heinrich, H. 1988. Origin and consequences of cyclic ice-rafting in the northeast Atlantic Ocean, during the past 130,000 yrs. *Quat. Res.*, 29: 143-152.

Huang, R. X. and R. L. Chou. 1994. Parameter sensitivity of the saline circulation. *Climate Dyn.*, 9: 391-409.

Huck, T., A. Colin de Verdiere, and A. J. Weaver. 1999. Interdecadal variability of the thermohaline circulation in box-ocean models forced by fixed surface fluxes. *J. Phys. Oceanogr.*, 29: 865-892.

Johnson, M. E., L. M. Moore, and D. Ylvisaker. 1990. Minimax and maximini distance designs. *J. Stat. Plan. Inf.*, 26: 131-148.

Kattenberg, A., F. Giorgi, H. Grassl, G. Meehl, J. Mitchell, R. Stouffer, T. Tokiada, A. Weaver, and T. Wigley. 1996. *Climate models – predictions of future climate*. In: Climate change 1995: The science of climate change. Cambridge University Press, Cambridge, UK, 549 p.

Keigwin, L. D., G. A. Jones, S. J. Lehman, and E.A. Boyle. 1991. Deglacial meltwater discharge, North Atlantic deep circulation, and abrupt climate change. *J. Geophys. Res.*, 96: 16,811-16,826.

Kushnir, Y. 1994. Interdecadal variations in North Atlantic Sea Surface Temperature and associated atmospheric conditions. *J. Climate*, 7: 141-157.

Lenderink, G. and R.J. Haarsma. 1994. Variability and multiple equilibria of the thermohaline circulation associated with deep water formation. *J. Phys. Oceanogr.*, 24: 1480-1493.

Lenderink, G. and R. J. Haarsma. 1996. Modeling convective transitions in the presence of sea-ice. *J. Phys. Oceanogr.*, 26(8): 1448-1467.

Lenderink, G. and R. J. Haarsma. 1999. On the mechanism of decadal oscillations in a coarse resolution ocean model. *Atmos.-Ocean*, 37(2): 179-202.

Levitus, S. 1982. *Climatological atlas of the world oceans*. NOAA Prof. Paper 13, Washington, D. C.

Manabe, S. and R. J. Stouffer. 1988. Two stable equilibria of a coupled ocean-atmosphere model. *J. Climate*, 1: 841-866.

Marotzke, J. 1989. Instabilities and steady states of the thermohaline circulation. *Oceanic Circulation Models: Combining Data and Dynamics*, D. L. T. Anderson and J. Willebrand, Eds., Kluwer, 501-511.

Marotzke, J. 1991. Influence of convective adjustment on the stability of the thermohaline circulation. *J. Phys. Oceanogr.*, 21: 903-907.

Marotzke, J. 1994. Ocean models in climate problems. *Ocean Processes in Climate Dynamics: Global and Mediterranean Examples*, P. Malanotte-Rizzoli and A. R. Robinson, Eds., Kluwer, 79-109.

Marotzke, J., P. Welander, and J. Willebrand. 1988. Instability and multiple steady states in a meridional-plane model of thermohaline circulation. *Tellus*, 40A: 162-172.

Marotzke, J. and J. Willebrand. 1991. Multiple equilibria of the global thermohaline circulation. *J. Phys. Oceanogr.*, 21: 1372-1385.

McKay, M., W. Conover, and R. Beckman. 1979. A comparison of three methods for selecting values of input variables in the analysis of output from computer code. *Technometrics*, 21: 239-245.

Mikolajewicz. U. and E. Maier-Reimer. 1990. Internal secular variability in an ocean general circulation model. *Climate Dyn.*, 4: 145-156.

Moore, A. M. and J. C. Reason. 1993. The response of a global ocean general circulation model to climatological surface boundary conditions for temperature and salinity. *J. Phys. Oceanogr.*, 23: 300-328.

Pacanowski, R., K. Dixon, and A. Rosati. 1991. The GFDL modular ocean model user guide. *GFDL Group Technical Report #2*, 44 p.

Pond, S. and G. L. Pickard. 1983. Introductory Dynamical Oceanography, Butterworth-Heinemann Ltd, 329 p.

Quon, C. and M. Ghil. 1992. Multiple equilibria in thermosolutal convection due to salt-flux boundary conditions. *J. Fluid Mech.*, 245: 449-483.

Quon, C. and M. Ghil. 1995. Multiple equilibria and stable oscillations in thermosolutal convection at small aspect ratio. *J. Fluid Mech.*, 291: 33-56.

Rahmstorf, S. 1994. Rapid climate transitions in a coupled ocean-atmosphere model. *Nature*, 372: 82-85.

Rahmstorf, S. 1995. Bifurcations of the Atlantic thermohaline circulation in response to changes in the hydrological cycle. *Nature*, 378: 145-149.

Rahmstorf, S. 1996. Comments on "Instability of the thermohaline circulation with respect to mixed boundary conditions: Is it really a problem for realistic models?" *J. Phys. Oceanogr.*, 26: 1099-1105.

Rahmstorf, S. and J. Willebrand. 1995. The role of temperature feedback in stabilizing the thermohaline circulation. *J. Phys. Oceanogr.*, 25: 787-805.

Rahmstorf, S., J. Marotzke, and J. Willebrand. 1996. Stability of the thermohaline circulation. In *The Warm Water Sphere of the North Atlantic Ocean*, edited by W. Krauss, Borntraeger, Stuttgart, Germany.

Reverdin, G., D. Cayan, and Y. Kushnir. 1997. Decadal variability of hydrography in the upper northern North Atlantic in 1948-1990. *J. Geophys. Res.*, 102: 8505-8531.

Roemmich, D. and C. Wunsch. 1984. Apparent changes in the climatic state of the deep North Atlantic Ocean. *Nature*, 307: 447-450.

Sacks, J., S. Schiller, and W. Welch. 1989. Designs for computer experiments. *Technometrics*, 31: 41-47.

Semtner, A. J., Jr. 1986. Finite difference formulation of a world ocean model. In *Advanced Physical Oceanographic Numerical Modeling*, edited by J. J. O'Brien, D. Reidel Publishing Company, 187-202.

Stommel, H. 1961. Thermohaline convection with two stable regimes of flow. *Tellus*, 13: 224-230.

Taylor, K. C., G. W. Lamoray, G. A. Doyle, R. B. Alley, P. M. Grootes, P. A., Mayewski, J. W. C. White, and L. K. Barlow. 1993. The "flickering switch" of late Pleistocene climate change. *Nature*, 361: 432-435.

Weaver, A. J., and T. M. C. Hughes. 1992. Stability and variability of the thermohaline circulation and its link to climate. *Trends in Physical Oceanography*, Research Trends Series, Council of Scientific Research Integration, 56 pp.

Weaver, A. J. and E. S. Sarachik. 1991a. The role of the mixed boundary conditions in numerical models of the ocean's climate. *J. Phys. Oceanogr.*, 21: 1470-1493.

Weaver, A. J. and E. S. Sarachik. 1991b. Evidence for decadal variability in an ocean general circulation model: An advective mechanism. *Atmos.-Ocean*, 29: 197-231.

Weaver, A. J., E. S. Sarachik, and J. Marotzke. 1991. Internal low frequency variability of the ocean's thermohaline circulation. *Nature*, 353: 836-838.

Weaver, A. J., J. Marotzke, P. F. Cummins, and E. S. Sarachik. 1993. Stability and variability of the thermohaline circulation. *J. Phys. Oceanogr.*, 23: 39-60.

Weaver, A. J., S. M. Aura, and P. G. Myers. 1994. Interdecadal variability in an idealized model of the North Atlantic. *J. Geophys. Res.*, 99: 12,423-12,441.

Welander, P. 1982. A simple heat salt oscillator. *Dyn. Atmos. Oceans*, 6: 233-242.

Welch, W., R. Buck, J. Sacks, H. Wynn, T. Mitchell, and M. Morris. 1992. Screening, predicting, and computer experiments. *Technometrics*, 34: 15-25.

Winton, M. 1995. Why is the deep sinking narrow? *J. Phys. Oceanogr.*, 25: 997-1005.

Winton, M. 1996. The role of horizontal boundaries in parameter sensitivity and decadal-scale variability of coarse-resolution ocean general circulation models. *J. Phys. Oceanogr.*, 26: 289-304.

Winton, M. 1997. The damping effect of bottom topography on internal decadal-scale oscillations of the thermohaline circulation. *J. Phys. Oceanogr.*, 27: 203-207.

Winton, M. and E. S. Sarachik. 1993. Thermohaline oscillations induced by strong steady salinity forcing of ocean general circulation models. *J. Phys. Oceanogr.*, 23: 1389-1410.

Wright, D. G. and T. F. Stocker. 1991. A zonally averaged ocean model for the thermohaline circulation. Part 1: Model development and flow dynamics, *J. Phys. Oceanogr.*, 21: 1713-1724.

Yin, F. and E. S. Sarachik. 1995. Interdeacadal thermohaline oscillations in a sector ocean general circulation model: advective and convective processes. *J. Phys. Oceanogr.*, 25: 2465-2484.

Yiou, P., M. Ghil, J. Jouzel, D. Paillard, and R. Vautard. 1994. Nonlinear variability of the climate system, from singular and power spectra of late Quaternary records. *Climate Dyn.*, 9: 371-389.

Yuen, C. W., J. Y. Cherniawsky, C. A. Lin, and L. A. Mysak. 1992. An upper ocean general circulation model for climate studies: global simulation with seasonal cycle. *Climate Dyn.*, 7: 1-18.

Zhang, S., R. J. Greatbatch, and C. A. Lin. 1993. A reexamination of the polar halocline catastrophe and implications for coupled ocean-atmosphere modeling. *J. Phys. Oceanogr.*, 23: 287-299.

Zhang, S., C. A. Lin, and R. J. Greatbatch. 1995. A decadal oscillation due to the coupling between an ocean model and a thermodynamical sea-ice model. *J. Mar. Res.*, 53: 79-106.